



# Design Approaches, Functionalization, and Environmental and Analytical Applications of Magnetic Halloysite Nanotubes: A Review

Meriem Fizir · Wei Liu · Xue Tang · Fangqi Wang · Yasmine Benmokadem

Accepted: 26 October 2022 / Published online: 17 November 2022  
© The Author(s), under exclusive licence to The Clay Minerals Society 2022

**Abstract** Researchers have long been committed to developing alternative, low-cost nanomaterials that have comparable capacity to carbon nanotubes. Halloysite nanotubes (HNTs) are naturally hollow, multi-walled, tubular structures that have high porosity, enlarged volumes and surface areas, and hydroxyl groups ready for modification. In addition, HNTs are non-toxic, biocompatible, inexpensive, abundant in nature, and easy to obtain. Magnetic nanocomposites have aroused widespread attention for their diverse potential applications in analytical fields and so magnetic halloysite nanotubes (MHNTs) have emerged as outstanding magnetic nano-adsorbent materials. Owing to their superparamagnetism, selective adsorption ability, and easy separation and surface modification, these captivating nanomaterials excel at extracting and enriching various analytes from environmental, biological, and food samples. The current review article gives an insight into recent advances

in the design, functionalization, characterization, and application of MHNTs as magnetic, solid-phase extraction sorbents for separation of antibiotics, pesticides, proteins, carcinogens such as polycyclic aromatic hydrocarbons (PAHs), dyes, radioactive ions, and heavy-metal ions in complex matrices.

**Keywords** Environmental applications · Functionalization · Halloysite nanotubes · Magnetic nanocomposites · Magnetic solid-phase extraction · Synthesis

## Introduction

Magnetic nanocomposites (MNCPs) have attracted widespread attention in analytical and biomedical fields, especially in sample pretreatment and drug-delivery systems, because of their magnetic properties, large specific surface areas, large pore volumes, rapid adsorption kinetics, and adjustable pore sizes (He et al., 2021; Shende & Shah, 2021; Zhu et al., 2013). In particular, the discovery of these nanomaterials has bestowed a tremendous impact on the development of analytical chemistry (Di et al., 2020). Generally, magnetic nanocomposites are base nanomaterials with embedded magnetic particles, which are oxides of metals such as Fe, Co, Ni, and Cu (Kharissova et al., 2015). Their superparamagnetism makes them ideally suited to overcome the challenges of time consumption of traditional solid-phase

Associate Editor: Lynda B. Williams

M. Fizir (✉) · Y. Benmokadem  
Laboratoire de Valorisation Des Substances Naturelles,  
Université Djilali Bounaâma, Khemis Miliana, Algérie  
e-mail: meriem.fizir@univ-dbk.m.dz; meriem\_fizir@163.com

M. Fizir · X. Tang · F. Wang  
Department of Chemistry, China Pharmaceutical  
University, Nanjing 211198, China

W. Liu  
Nanjing Institute for Comprehensive Utilization of Wild  
Plants, Nanjing, China

extraction (SPE) systems and to simplify dramatically the pretreatment procedure and improve the extraction efficiency by employing magnetic separation (Yu et al., 2019). Moreover, MNCPs have been developed to avoid the limitation of specific surface area and drawbacks of agglomeration which result in weakened and leaky magnetism of magnetic nanoparticles (MNPs) such as iron oxides when they have been used as sole particles (Rios et al., 2013).

Research has continued apace to search for and develop novel MNCPs as adsorbents which have large adsorption capacities. Carbon-based materials or porous materials with various morphologies have been embedded with MNPs to form MNCPs, e.g. graphene oxide (GO) (Farooq & Jalees, 2020), carbon nanotubes (CNTs) (Gao et al., 2006), and metal–organic frameworks (MOFs) (Kurmoov, 2009). All these nanocomposites not only have superparamagnetic properties, large specific surface areas, and large adsorption capacities but also enhanced recovery from the reaction medium (Farooq & Jalees, 2020). However, their cost and toxicity are major concerns. To be specific, GO and CNTs should not be applied without carboxylation, and their significant toxicity could be addressed by biocompatible polymer modification (Itatahine et al., 2017). In addition, the aforementioned nanomaterials are not available in nature, which means they are produced using specialized experimental protocols which are laborious and time consuming. To overcome these problems, researchers have sought to develop alternative low-cost nanomaterials that possess comparable capacities to CNTs or GO. Recently, as a low-cost and naturally available biocompatible material, halloysite nanotubes (HNTs) have attracted rapidly growing interest (Li et al., 2022).

Nanosized tubular halloysites are naturally hollow, multi-walled tubular structures. Transmission electron microscopy (TEM) analysis showed that the length of HNTs is within the micrometer range (0.4–1  $\mu\text{m}$ ), the inner lumen diameters are 10–70 nm, and the outer diameter is 20–200 nm (Yu et al., 2016). The unitary cell formula is  $\text{Al}_2\text{Si}_2\text{O}_5(\text{OH})_4 \cdot n\text{H}_2\text{O}$ . HNTs have large porosity, enlarged volume and surface area, and plenty of hydroxyl groups available for modification (Zhang et al., 2016). In addition, HNTs are available and abundant in nature, non-toxic, biocompatible, and cheap (Yendluri et al., 2017). HNTs are composed of a gibbsite-like array of aluminol (Al–OH)

groups in the inner space of the lumen, and siloxane (Si–O–Si) groups on the outer surface (Fig. 1a) (Fizir et al., 2018a). This distinctive structural composition offers HNTs a negatively charged outer surface and a positively charged inner lumen, over a broad range of pH values (Joussein et al., 2005; Lvov et al., 2008). The unique surface chemistry of HNTs can be similarly anchored with MNPs such as  $\text{Fe}_3\text{O}_4$  to yield a promising framework for magnetic nanoparticles (Duan et al., 2012). In recent years, magnetic halloysite nanotubes (MHNTs), derivative nanocomposites from low-cost halloysites, have shown promise for future use in magnetic solid-phase extraction for the enrichment of various analytes from environmental, biological, and food samples. For example, coating HNTs with MNPs enhanced the removal capacity of heavy metals such as arsenic, cadmium, and lead (Maziarz & Matusik, 2017). The trend in terms of published articles about MHNTs since their discovery is shown in Fig. 1b. Most of the cited articles have been published since 2018. Obviously, research on MHNTs is still in its infancy and there seem to be no specialized reviews about the methods of preparation of MHNTs or their analytical applications. Therefore, a summary review on magnetic halloysite nanotubes from preparation to application is of importance in this field.

Indeed, many similar reviews have been published on the subject of the properties and application of halloysite in various fields including analytical chemistry and in environmental and biomedical applications (Fakhrullin & Lvov, 2016; Fizir et al., 2018a, 2020; Lvov et al., 2016; Naumenko et al., 2016), where the common methods of preparation of magnetic halloysite nanotubes were highlighted. However, detailed synthesis strategies, functionalization, and application of HNTs combined with magnetic nanoparticles have not been reviewed. The present review starts with the synthetic strategies of MHNTs. Coating HNTs with MNPs can be categorized into in situ growth, nano-encapsulation, and direct-mixing methods. Some novel methods are presented for the first time. The advantages and limitations of each approach are summarized critically and, based on the authors' understanding of the subject, some solutions for preparing MHNTs with superior characteristics are recommended. Then, the structural characteristics of synthesized MHNT nanocomposites are described briefly. Furthermore,

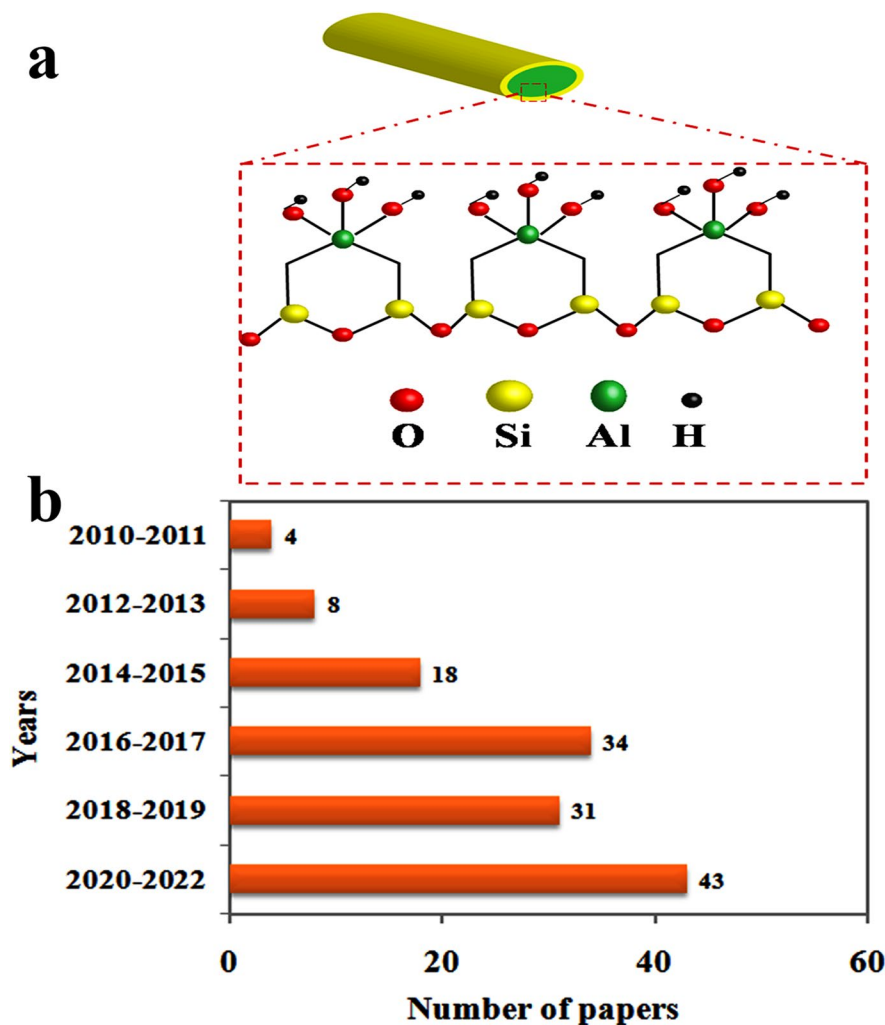


**Fig. 1** **a** Schematic illustration of the crystalline structure of HNTs, and **b** Growth trend of number of articles on MHNTs published during 2010–2022 (data analysis done in September 2022)

functionalization approaches of MHNTs with various kinds of organic and inorganic molecules such as polymers, silane agents, and ionic liquids are highlighted. After that, the analytical applications of designed MHNT nanocomposites are summarized. In this part, the focus is on the application of composites as magnetic adsorbents in magnetic solid phase extraction (MSPE) for the separation of antibiotics, pesticides, proteins, carcinogens such as polycyclic aromatic hydrocarbons (PAHs), dyes, radioactive ions, and heavy-metal ions such as Cu(II), Cd(II), Pb(II), Hg(II), Cr(III), and Cr(VI) in complex matrices (Fig. 2a). Finally, current challenges and speculation about the potential ongoing

exploration of MHNT nanocomposites for analytical achievements are discussed.

### Preparation methods of MHNTS

The magnetic nanoparticles used most commonly for the preparation of MHNTs are metals, metal oxides, or ferrites such as ferromagnetic or superparamagnetic iron oxides [e.g. magnetite ( $\text{Fe}_3\text{O}_4$ ) and ferric oxide ( $\gamma\text{-Fe}_2\text{O}_3$ )] (Majidi et al., 2016). MHNT particles are produced mainly by chemical synthesis which includes various processes such as co-precipitation, in situ precipitation, wet impregnation, solvothermal,

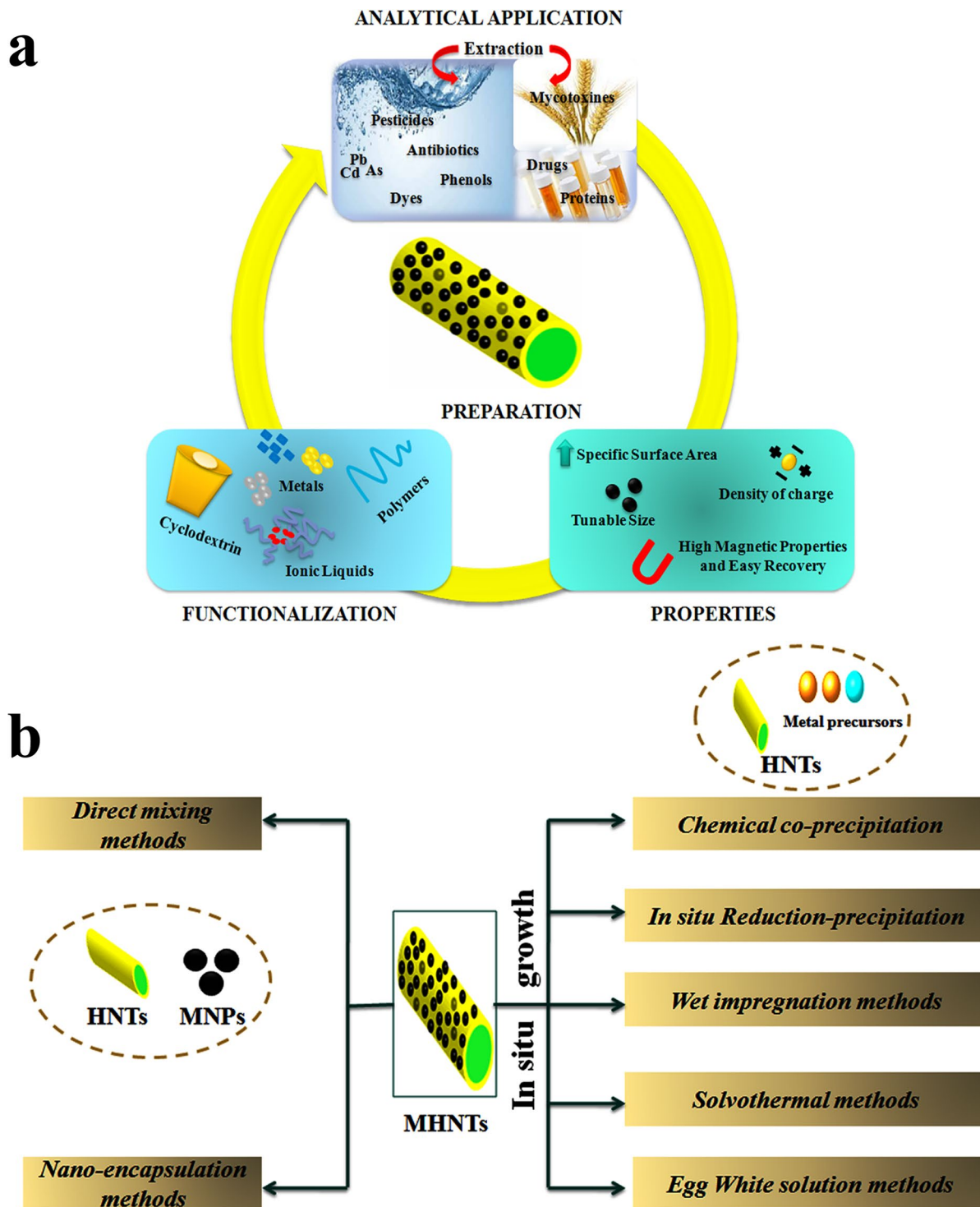


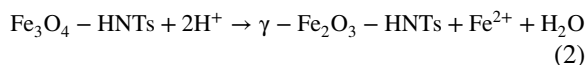
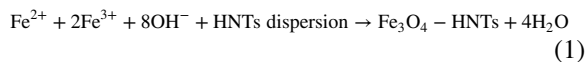
**Fig. 2** **a** Preparation, properties, and functionalization of MHNT composites and their analytical applications, and **b** summary of the synthesis methods for MHNT composites

egg-white solution, nano-encapsulation, and direct-mixing methods (Fig. 2b). All the above-mentioned methods except loading and direct-mixing approaches are in situ growth methods because the formation of MNPs is carried out in the presence of the HNTs. Among them, chemical co-precipitation is the most commonly employed method, and its synthetic methods are steerable under mild conditions (Chen et al., 2016).

### Chemical Co-precipitation Method

Co-precipitation is a simple, controllable, and low-cost technique (He et al., 2021). The method consists of dissolving a stoichiometric mixture of iron salts (e.g.  $\text{FeCl}_3 \cdot 6\text{H}_2\text{O}$  and  $\text{FeSO}_4 \cdot 7\text{H}_2\text{O}$  or  $\text{FeCl}_2 \cdot 4\text{H}_2\text{O}$ ) in deionized water, introducing a pre-treated HNT dispersion, and adjusting the dispersion medium in the pH range of 9–13 with base (Eq. 1) in the presence of nitrogen gas to prevent the critical oxidation of  $\text{Fe}_3\text{O}_4$  into  $\gamma\text{-Fe}_2\text{O}_3$  (Eq. 2) (Fizir et al., 2018a; Konnova et al., 2016). In this method, the nucleation and growth of magnetic nanoparticle nuclei occur in situ in an aqueous dispersion of HNTs (López-López et al., 2005). Thus, the iron oxide nanoparticles precipitate with HNT particles and form  $\text{Fe}_3\text{O}_4$ -HNTs nanocomposites. The mechanism of  $\text{Fe}_3\text{O}_4$ -HNT formation is based on the electrostatic interaction between MNPs and HNTs where the cationic-metal ion precursors of  $\text{Fe}_3\text{O}_4$  nanoparticles become attached to the negatively charged HNTs (Abhinayaa et al., 2018). Another explanation is that the metal ions could be adsorbed and retained in the large pore volume of HNTs (Afzali & Fayazi, 2016). By using the co-precipitation method, a high yield of MHNTs could be obtained. However, the main drawbacks of this method are the uncontrollable size distribution and the possibility of leakage of MNPs, which are challenging issues (Chen et al., 2016). For example, MHNTs have been prepared with MNPs ranging in size from 10 to 16 nm (Fizir et al., 2017, 2018b; Li et al., 2018a). In a study conducted by Liang et al. (2021), the size of  $\text{Fe}_3\text{O}_4$  attached to HNTs nanoparticles was ~20–50 nm where a smaller subunits comprising MNPs of ~10 nm were found by Xie et al. (2011). These different MNP sizes can be explained as follows: nuclei should be isolated during the period of growth to obtain a very narrow size distribution of the monodispersed NPs produced. Evidently, in

the system containing MNP and HNT dispersions, the two phases cannot be separated easily. Worth mentioning is that for MSPE application, the size of MNPs attached to HNTs is not very important as in pharmaceutical (drug-delivery system) or catalysis applications where the size of the metal NPs should be controlled precisely (Gao et al., 2020). Consequently, the method of choice may depend on the target application of the nanocomposites. Another point that researchers should be aware of during synthesis of MHNTs is the mass ratio of the total iron salts ( $\text{Fe}^{2+}$ :  $\text{Fe}^{3+}$ ) to HNTs. A large amount of  $\text{Fe}_3\text{O}_4$  particles could aggregate together when the mass ratio is > 3:1. In addition, when the ratio 2:1 or 3:1 is used, a unique cactus-like  $\text{Fe}_3\text{O}_4$ -HNT is produced. The acicular  $\text{Fe}_3\text{O}_4$  on HNTs can develop into granular  $\text{Fe}_3\text{O}_4$  as the time is extended to 24 h rather than 4 h (Song et al., 2019). In addition, the high ratio can have a negative effect on the adsorption of analytes (Wan et al., 2017). In order to satisfy the goal of magnetic separation without affecting the adsorption capacity of the nanocomposites, a ratio in the range of 1:1 to 3:1 and 4 h of agitation to prepare MHNTs is recommended. Agitation speed is also an important parameter that can affect the final size of MNPs and needs to be controlled during the preparation of MHNTs.



### In Situ reduction-precipitation Method

The MHNTs are synthesized via in situ reduction of metal precursors on the surface of HNTs (Jia et al., 2011; Kadam et al., 2020b; Lee et al., 2019). For magnetic materials, metal precursors, e.g.  $\text{FeCl}_3$ , bind with HNT surfaces for electrostatic interactions between positive charges of metal ions and external negatively charged HNT. With the help of reductants such as  $\text{Na}_2\text{SO}_3$  and  $\text{NaBH}_4$ , magnetic nanoparticles were synthesized on HNT surfaces in situ (Jee et al., 2020; Jiang et al., 2014b; Kim et al., 2018; Lee et al., 2019). The formation strategy was that some  $\text{Fe}^{3+}$  ions in the solution were reduced to  $\text{Fe}^{2+}$  by  $\text{Na}_2\text{SO}_3$  or  $\text{NaBH}_4$ . Finally, the iron oxide nanoparticles were

formed homogeneously with the addition of base (NaOH). This method is simpler, faster, and cheaper (Jee et al., 2020; Jiang et al., 2014b; Kim et al., 2018; Lee et al., 2019). Note that the sizes of MNPs prepared by this method were difficult to control (Table 3) (Li et al., 2020a) and that the use of reductants may increase the cost of the method.

### Wet Impregnation Method

Wet impregnation, employing a physical mixture of the HNTs in a solid state and the MNPs dissolved in a liquid solution, is the simplest method for loading a given porous support as HNT (Tušar et al., 2013). This method consists of a dispersion of a known amount of HNT with a metal ion precursor (e.g.  $\text{Fe}(\text{NO}_3)_3 \cdot 9\text{H}_2\text{O}$ ) in the solvent. After drying and removing the excess solvent, e.g. ethanol or methanol, the solid powder obtained is impregnated with ethylene glycol and subjected to thermal treatment (calcination) under a nitrogen atmosphere (Cheng et al., 2019; Hang et al., 2013; Ma et al., 2016a; Tsoufis et al., 2017). The formation process is that the positive  $\text{Fe}^{2+}$  and  $\text{Fe}^{3+}$  ions are introduced onto HNT surfaces through complexation reactions under agitation and  $\text{Fe}_3\text{O}_4$  nanoparticles (or Cu/Co  $\text{Fe}_2\text{O}_4$  NPs) are loaded into HNTs after high-temperature calcination (Hang et al., 2013; Maleki et al., 2019; Pan et al., 2012a; Zhang et al., 2020). The average size of the  $\text{Fe}_3\text{O}_4$  NPs ranged from 5 to 36 nm (Table 1) (Dai et al., 2014; Gan et al., 2015; He et al., 2016a, 2016b; Tsoufis et al., 2017; Zeng et al., 2016).

It is widely recognized that the pore size of HNTs decreased with increasing temperature ( $>300^\circ\text{C}$ ) (Mu et al., 2014a). It is difficult, therefore, to insert metals and metal oxides into HNT lumens without damaging the structure of the HNT (Table 3). This drawback may be resolved by decreasing the calcination temperature to  $<300^\circ\text{C}$  and increasing the calcination time.

### Solvothermal Method

The solvothermal process is considered to be among the most promising approaches to producing MHNTs. The thermal decomposition of the precursor is the principle of the method (Fizir et al., 2018a). This technique consists of dissolving ethylene glycol (EG) as an organic solvent with a specific percentage of the iron precursor solution (i.e.  $\text{FeCl}_2$  or  $\text{FeCl}_3$ ), dispersing HNTs in this solution, and adjusting the pH through the addition of an alkaline solution. Then, the mixture may undergo crystallization in a high-temperature and pressure reactor (Mirbagheri & Sabbaghi, 2018; Pan et al., 2011, 2012a). In the solvothermal preparation, MHNTs are synthesized via a Teflon-lined stainless steel autoclave under high temperature of  $195\text{--}200^\circ\text{C}$  and pressure of  $3 \times 10^{-9}\text{--}4 \times 10^{-8}$  bar (Jia et al., 2016, 2017; Tian et al., 2016; Zhou et al., 2016). The formation mechanism is that  $\text{Fe}^{3+}$  or  $\text{Fe}^{2+}$  ions are adsorbed on the surface of HNTs through electrostatic attraction and then reduced to  $\text{Fe}_3\text{O}_4$  or  $\gamma\text{-Fe}_2\text{O}_3$  by ethylene glycol.

**Table 1** Synthesis conditions, saturation magnetization (Ms), and the size of MNPs of the MHNTs prepared using wet impregnation

Precursors	MNPs-HNTs	Calcination $T$ ( $^\circ\text{C}$ )	Size (nm)	Ms ( $\text{emu g}^{-1}$ )	References
$\text{Fe}(\text{NO}_3)_3 \cdot 9\text{H}_2\text{O}$ and $\text{Cu}(\text{NO}_3)_2 \cdot 3\text{H}_2\text{O}$	$\text{CuFe}_2\text{O}_4$ -HNTs	500	35.88	30.00	(Maleki et al., 2019)
$\text{Fe}(\text{NO}_3)_3 \cdot 9\text{H}_2\text{O}$ and $\text{Co}(\text{NO}_3)_2 \cdot 6\text{H}_2\text{O}$	$\text{CoFe}_2\text{O}_4$ -HNTs	600	5.0–10	18.98	(Pan et al., 2012a)
$\text{Fe}(\text{NO}_3)_3 \cdot 9\text{H}_2\text{O}$ and $\text{Co}(\text{NO}_3)_2 \cdot 6\text{H}_2\text{O}$	$\text{CoFe}_2\text{O}_4$ -HNTs	750	9–10	–	(Zhang et al., 2020)
$\text{Fe}(\text{NO}_3)_3 \cdot 9\text{H}_2\text{O}$	$\text{Fe}_3\text{O}_4$ -HNTs	400	12	2.85	(Dai et al., 2014)
$\text{Fe}(\text{NO}_3)_3 \cdot 9\text{H}_2\text{O}$	$\text{Fe}_3\text{O}_4$ -HNTs	400	11	2.85	(He et al., 2016a)
$\text{Fe}(\text{NO}_3)_3 \cdot 9\text{H}_2\text{O}$	$\text{Fe}_3\text{O}_4$ -HNTs	400	10	7.00	(Zeng et al., 2016)
$\text{Fe}(\text{NO}_3)_3 \cdot 9\text{H}_2\text{O}$	$\text{Fe}_3\text{O}_4$ -HNTs	400	10–13	6.00	(Cheng et al., 2019)
$\text{Fe}(\text{NO}_3)_3 \cdot 9\text{H}_2\text{O}$	$\text{Fe}_3\text{O}_4$ -HNTs	265	5–8	2.19	(Gan et al., 2015)
$\text{Fe}(\text{NO}_3)_3 \cdot 9\text{H}_2\text{O}$	$\text{Fe}_3\text{O}_4$ -HNTs	265	10	2.41	(Hang et al., 2013)
$\text{Fe}(\text{NO}_3)_3 \cdot 9\text{H}_2\text{O}$	$\text{Fe}_3\text{O}_4$ -HNTs	400	11	2.81	(Ma et al., 2016a)
$\text{Fe}(\text{NO}_3)_3 \cdot 9\text{H}_2\text{O}$	$\text{Fe}_3\text{O}_4$ -HNTs	200	15	–	(Tsoufis et al., 2017)

High-temperature conditions are beneficial for improving magnetism, which are the main advantage of this synthesis technique. In addition, the properties of the MHNTs, including size, density, and crystallinity of MNPs, can be changed through modification of the solvothermal reaction conditions such as temperature, time, concentrations, and the ratio of reactants (He et al., 2021). The average size of the  $\gamma$ -Fe<sub>2</sub>O<sub>3</sub> and Fe<sub>3</sub>O<sub>4</sub> NPs attached to HNTs prepared by this method range from 20 to 200 nm (Table 2) (Mirbagheri & Sabbaghi, 2018; Pan et al., 2012b). Although this method forms a tunable morphology of MNPs attached to HNTs with high magnetism, it is expensive (Table 3).

### Egg-White Solution-assisted Thermal Method

A cost-effective method is to use egg white solutions to synthesize NiFe<sub>2</sub>O<sub>4</sub>-HNTs nanoparticles. This process consists of dispersing Ni(NO<sub>3</sub>)<sub>2</sub>·6H<sub>2</sub>O, Fe(NO<sub>3</sub>)<sub>3</sub>·9H<sub>2</sub>O, and freshly extracted egg white (ovalbumin) as precursors and HNTs in an aqueous medium. Afterward, the resulting dried precursors were calcined at 700°C to form desired crystalline NPs (Zare Pirhaji et al., 2020a, 2020b). Egg white is used due to its aqueous solubility and its ability to bind with metal ions (Gabal, 2010). Therefore, egg-white solution acts as a good surfactant to reduce the impurities in the prepared composites (Gabal et al., 2012; Maensiri et al., 2007). There are

**Table 2** Synthesis conditions, saturation magnetization (Ms), and the size of MNPs of the MHNTs prepared by the solvothermal method

Precursors/Organic solvent (ratio of precursors to HNTs)	Calcination		MNPs-HNTs	Size (nm)	Ms (emu g <sup>-1</sup> )	Reference
	T (°C)	Time (h)				
FeCl <sub>2</sub> /EG (1:1)	200	24	$\gamma$ -Fe <sub>2</sub> O <sub>3</sub> -HNTs	20	9.78	(Mirbagheri & Sabbaghi, 2018)
FeCl <sub>3</sub> ·6H <sub>2</sub> O/EG (3:1)	200	8	Fe <sub>3</sub> O <sub>4</sub> -HNTs	200	47.31	(Jia et al., 2016)
FeCl <sub>3</sub> ·6H <sub>2</sub> O/EG (1:2)	200	8	Fe <sub>3</sub> O <sub>4</sub> -HNTs	75	36.99	(Wang, P., et al., 2012)
FeCl <sub>3</sub> ·6H <sub>2</sub> O/EG (3:1)	200	8	Fe <sub>3</sub> O <sub>4</sub> -HNTs	100	42.71	(Zhou et al., 2016)
FeCl <sub>3</sub> ·6H <sub>2</sub> O/EG (3:1)	200	8	Fe <sub>3</sub> O <sub>4</sub> -HNTs	150	36.5	(Jia et al., 2017)
FeCl <sub>3</sub> ·6H <sub>2</sub> O/EG (1.3:1)	200	8	Fe <sub>3</sub> O <sub>4</sub> -HNTs	–	24.5	(Tian et al., 2016)

**Table 3** Summary of the characteristics of common synthetic strategies of MHNTs (Chen et al., 2016; Li et al., 2020a; Mu et al., 2014a)

Method	Advantages	Disadvantages
Chemical co-precipitation method	<ul style="list-style-type: none"> <li>• Short synthesis time</li> <li>• High productivity</li> <li>• Retain a complete structure of the HNTs</li> <li>• Use less harmful products</li> </ul>	<ul style="list-style-type: none"> <li>• Uncontrollable size distribution</li> <li>• Possibility of MNP leakage</li> <li>• Purification steps for adjusting the pH of the mixture</li> </ul>
In situ reduction-precipitation method	<ul style="list-style-type: none"> <li>• Short synthesis time (&lt;2 h)</li> </ul>	<ul style="list-style-type: none"> <li>• Uncontrollable size distribution</li> </ul>
Wet impregnation	<ul style="list-style-type: none"> <li>• The small size of MNPs</li> </ul>	<ul style="list-style-type: none"> <li>• Possibility of damage to the structure of lumen of the HNTs</li> </ul>
Solvothermal method	<ul style="list-style-type: none"> <li>• High crystallinity</li> <li>• Tunable morphology of MNPs</li> <li>• High magnetism</li> <li>• Good dispersibility in organic solvents</li> </ul>	<ul style="list-style-type: none"> <li>• Long reaction time</li> <li>• Require more solvents</li> <li>• Cost</li> <li>• Low productivity</li> <li>• Big size of the MNPs</li> </ul>
Egg white solution-assisted thermal method	<ul style="list-style-type: none"> <li>• High crystallinity</li> <li>• No solvents/green synthesis</li> </ul>	<ul style="list-style-type: none"> <li>• Possibility of damage to the structure of the HNT lumen</li> </ul>
Nano-encapsulation method	<ul style="list-style-type: none"> <li>• Incorporating MNPs with different sizes</li> <li>• Stability of the composite</li> </ul>	<ul style="list-style-type: none"> <li>• Functionalization of MNPs and HNTs</li> <li>• Reduction in specific surface area</li> </ul>
Direct mixing method	<ul style="list-style-type: none"> <li>• Simple strategy</li> </ul>	<ul style="list-style-type: none"> <li>• MNPs are easily detached from HNTs</li> </ul>

two main limitations of the aforementioned methods based on in situ growth of MNPs: one is that the selected HNTs must remain stable under the precursor mixture of  $\text{Fe}_3\text{O}_4$  nanoparticles; the other is that it is possible to generate free MNPs in solution (Table 3).

### Nano-Encapsulation Method

Coating MNPs onto the mesoporous HNTs could also be achieved by a nano-encapsulation-based approach. This method uses mainly functionalization of the inner lumen of HNT to promote the growth of MNPs into the inner channels to prepare MHNTs (first approach) or loading modified MNPs by a vacuum method (second approach). In the first approach, HNTs are modified to make the alumina core hydrophobic. Metal oleate (Zhang et al., 2014), tetradecylphosphonic acid (Hamza et al., 2020), and urease (Zheng et al., 2015) are used for hydrophobic modification. Once the iron ions diffuse into HNTs,  $\text{Fe}_3\text{O}_4$  grows in the HNTs to obtain  $\text{Fe}_3\text{O}_4$ -HNTs nano-encapsulates. Metal oleate is used as a ferrite precursor and for the hydrophobic modification of HNTs also. By using this strategy, the metal oleate complex entered into the inner space of the HNTs, and ferrite nanoparticles are then formed in situ during the subsequent heat treatment (Zhang et al., 2014). HNTs are loaded with urease and impregnated metal ion precursor with urea solution. The loaded urease hydrolyzed urea to produce  $\text{NH}_3$  and iron ions are grown in situ (Fig. 3a) (Zheng et al., 2015).

In the second approach, the prepared MNPs of diameter  $\sim 6$  nm are functionalized and subsequently added to the modified HNTs by using repeated vacuum/ $\text{N}_2$  cycles while stirring. By using this strategy, all MNPs can be loaded into the lumen of HNTs without any relevant interaction with the HNT outer surface (Fig. 3b) (Hamza et al., 2020). This method not only has the unique advantage of incorporating MNPs with various sizes but also enables the construction of MNCPs in a controllable manner, and their migration could be suppressed significantly due to the spatial confinement which accounts for high composite stability. The main drawback of this approach is the time consumed in the functionalization of both guests – HNTs and MNPs (Table 3).

### Direct Mixing Method (self-assembly)

Mixing HNTs and MNPs directly is a simple strategy to design MHNTs which is completed by the self-assembly of MNPs on the surfaces of HNTs (Khunová et al., 2016, 2018) or vice versa, which means the attachment of HNTs on the surface of iron oxide microspheres depends on the size of the MNPs (Duan et al., 2021). Uniform mixing of previously functionalized or prepared MNPs and HNTs is carried out under ultrasonication or stirring (Duan et al., 2021; Pan et al., 2014). The preparation of MHNTs by direct mixing relies on electrostatic interactions and covalent bonding. Based on this, a halloysite-encapsulated magnetic microsphere composite is prepared by ultrasonication of the mixture of  $\text{Fe}_3\text{O}_4$ - $\text{SiO}_2$  and Cu-HNTs (Fig. 4a). The silica layer is employed commonly to coat MNPs in the mixing method, which can greatly improve the reactivity of MNPs and the stability of MHNTs (Duan et al., 2021). The self-assembly of Lys- $\text{Fe}_3\text{O}_4$  on the surface of Ag/HNTs is carried out by a simple mixing technique. Lys- $\text{Fe}_3\text{O}_4$  nanoparticles with the protonated amino groups are easily embedded in the surface of Ag/HNTs via electrostatic interaction (Fig. 4b). Ag/HNTs/ $\text{Fe}_3\text{O}_4$  nanocomposites show high saturation magnetization values of  $24.27 \text{ emu g}^{-1}$  (Mu et al., 2014a). The same strategies are followed to prepare Au/HNTs/ $\text{Fe}_3\text{O}_4$  (Mu et al., 2014b). In other research, poly glycidyl methacrylate-grafted MNPs (MNPs-g-PGMA) are deposited on the surfaces of HNT- $\text{NH}_2$  by a simple mixing technique. The formation mechanism is based on the chemical reaction between epoxy rings of the PGMA chains and amino groups of the HNTs (Nguyen et al., 2017). The method of direct mixing of  $\text{Fe}_3\text{O}_4$  NPs and hydrothermally carbonized glucose on HNTs (HNTs-Glu) was developed recently. HNTs-Glu-Fe showed high superparamagnetic properties of  $50.7 \text{ emu g}^{-1}$  (Sadjadi et al., 2019).

### Structural Characterizations of MHNTs

Various physicochemical identification techniques have been used to examine the structural and distinctive features of the synthesized MHNTs, e.g. Fourier-transform infrared spectroscopy (FTIR), Raman spectroscopy, X-ray diffraction (XRD), vibrating sample magnetometry (VSM), energy-dispersive spectrometry



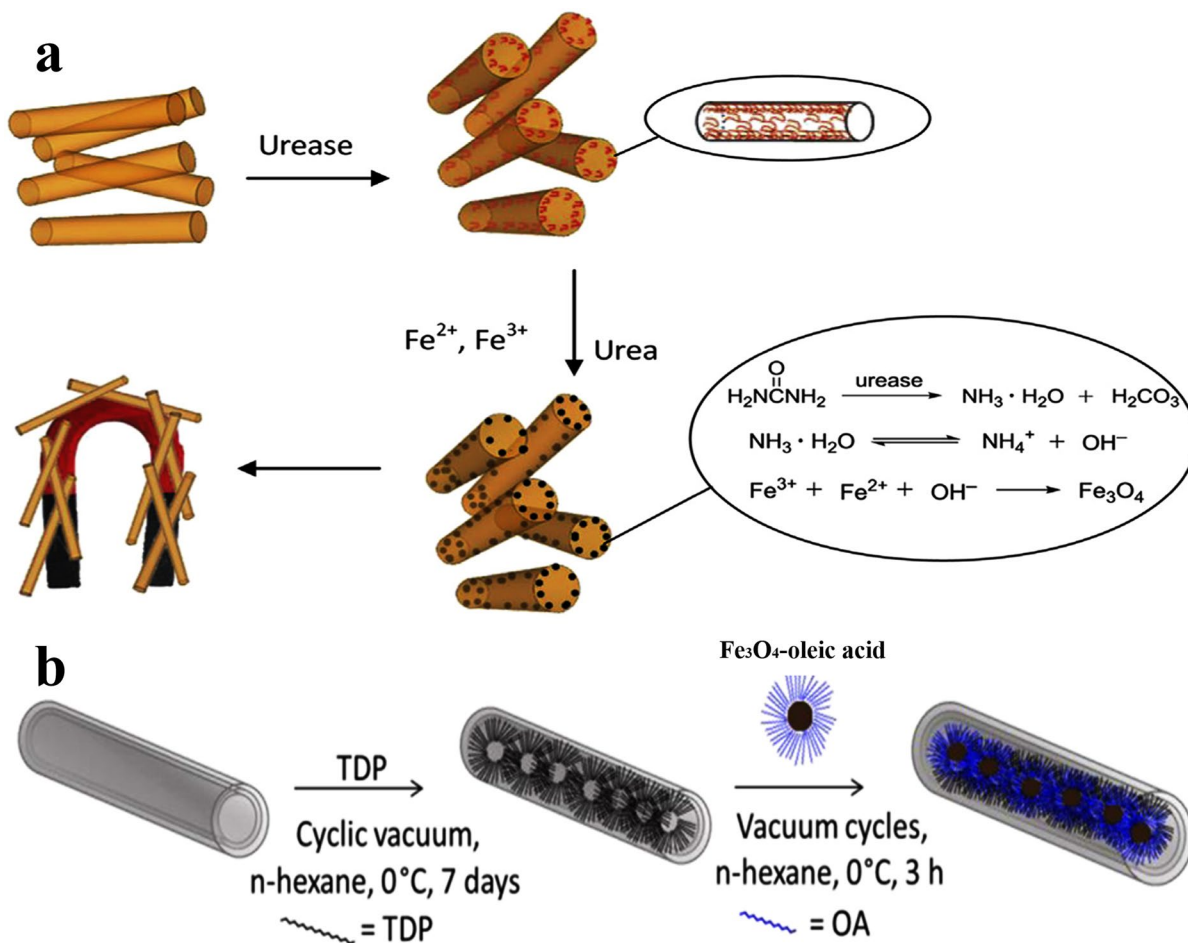


**Fig. 3** Encapsulation approaches of  $\text{Fe}_3\text{O}_4$  into the lumens of HNTs: **a** urease immobilization and  $\text{Fe}_3\text{O}_4$  formation in the lumens of HNTs (reproduced from Zheng et al., (2015) with the permission of Elsevier), and **b** selective loading of  $\text{Fe}_3\text{O}_4$  in the inner part of HNTs (reproduced from Hamza et al.(2020) with permission of the ACS)

(EDS), transmission electron microscopy (TEM), and scanning electron microscopy (SEM). FTIR spectroscopy is used to confirm the presence of expected functional groups. The absorption peak at  $1030\text{ cm}^{-1}$  is from the Si–O groups in MHNTs. The peaks at  $536$  and  $912\text{ cm}^{-1}$  are characteristic of Al–O–Si and the internal hydroxyl group vibrations, respectively, in magnetic nanotubes. The peak at  $3430\text{ cm}^{-1}$  is due to structural O–H stretching vibrations from iron oxides of MHNTs. The FTIR analyses showed that the bands of the Al–O–Si of HNTs at  $536$  or  $540\text{ cm}^{-1}$  and characteristic MNP peaks at  $580\text{ cm}^{-1}$  are overlapped in MHNTs (Amjadi et al., 2015a; Fizir et al., 2017; Hajizadehet al., 2020a). To identify the crystalline structure of MHNTs, XRD examinations are

used. The XRD traces display distinct peaks in the range  $30\text{--}65^\circ 2\theta$  which can be indexed as (220), (311), (400), (422), (511), and (440). These peaks are in accordance with the crystalline cubic system of iron oxide NPs (Bilici et al., 2020; Maleki et al., 2018; Xie et al., 2011). The magnetic behavior of MHNTs is examined using VSM. The saturation magnetization value could be observed through the magnetization of MHNTs as a function of the applied magnetic field (sweeping from  $-1$  to  $1$  T) curve at room temperature ( $25^\circ\text{C}$ ). The magnetization increases with increase in the magnetic field. MHNTs possess superparamagnetic properties with saturation magnetization ranging from  $21$  to  $50\text{ emu g}^{-1}$  (Hajizadeh et al., 2020b; He et al., 2016a, 2016b; Shi et al., 2020). Saturation

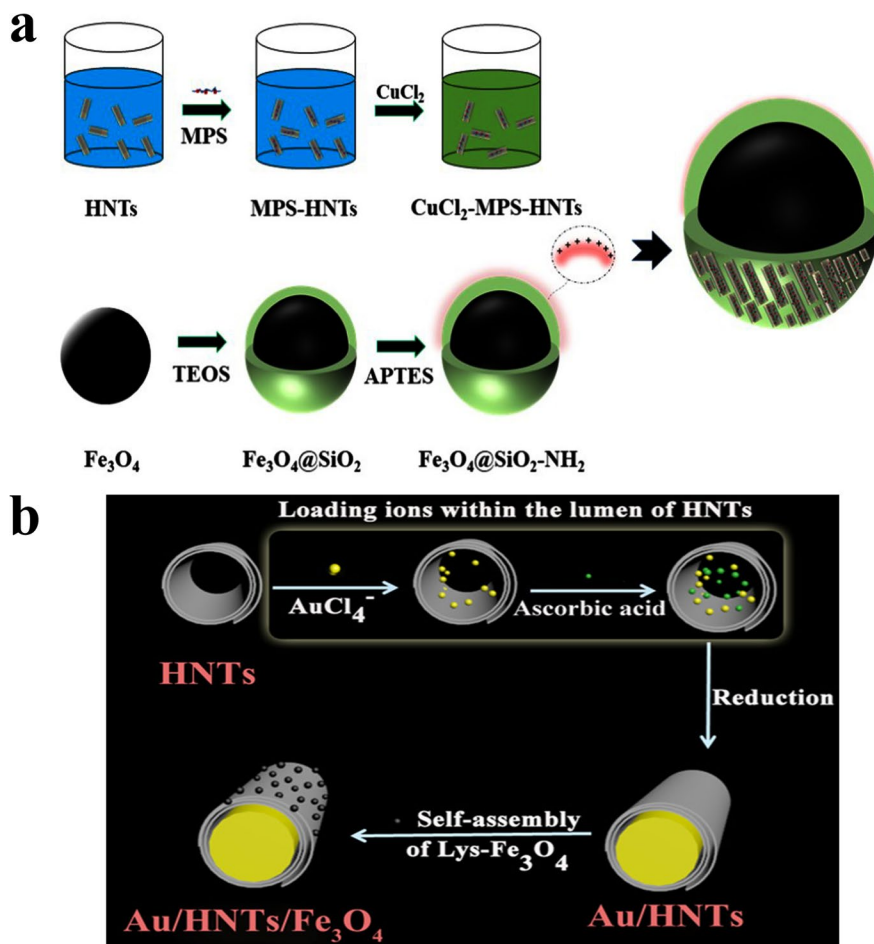


**Fig. 4** MHNTs prepared using direct mixing methods: **a** the preparation process of  $\text{Fe}_3\text{O}_4@SiO_2@Cu$ -MHNTs (reproduced from Duan et al. (2021) with the permission of Elsevier) and **b** schematic illustration of the preparation of  $Au/HNTs/Fe_3O_4$  (reproduced from Mu et al., 2014a with the permission of the Royal Society of Chemistry)

magnetization depends on the synthesis conditions and on the size of the MNPs (He et al., 2021). The chemical composition of MHNTs is investigated using EDS where very strong signals of Fe, O, Al, and Si are observed in the MHNTs (Dramou et al., 2018; Hajizadeh, et al., 2020a; Shi et al., 2020). The TEM and SEM analyses are used to examine the morphological structure and diameter of MHNTs. The incorporation of MNPs does not affect or modify the morphology of the HNTs (Zhu et al., 2021). Typically, the diameter of MNPs and their surface morphology depend on the design approach and experimental conditions. In the present review, the morphology of the prepared MHNTs by different synthesis methods are discussed.

For example, in the MHNTs prepared by co-precipitation methods, the MNPs were deposited and attached to the external surface of HNTs with diameters ranging from 5 to 50 nm. As shown in Fig. 5a, the size of iron oxide particles is ~16 nm (Fizir et al., 2017; Li et al., 2018b). The same morphology was observed for MHNTs prepared by solvothermal methods (Fig. 5b) (Pan et al., 2011) and direct mixing methods (Fig. 5c) (Mu et al., 2014b). However, the size of MNPs formed by thermal decomposition (range 75 to 200 nm) is larger than that from co-precipitation (Fig. 5d). For MHNTs prepared by the wet impregnation technique, it was noted that MNPs were distributed on the inside surfaces of HNTs with diameters ranging from 5 to

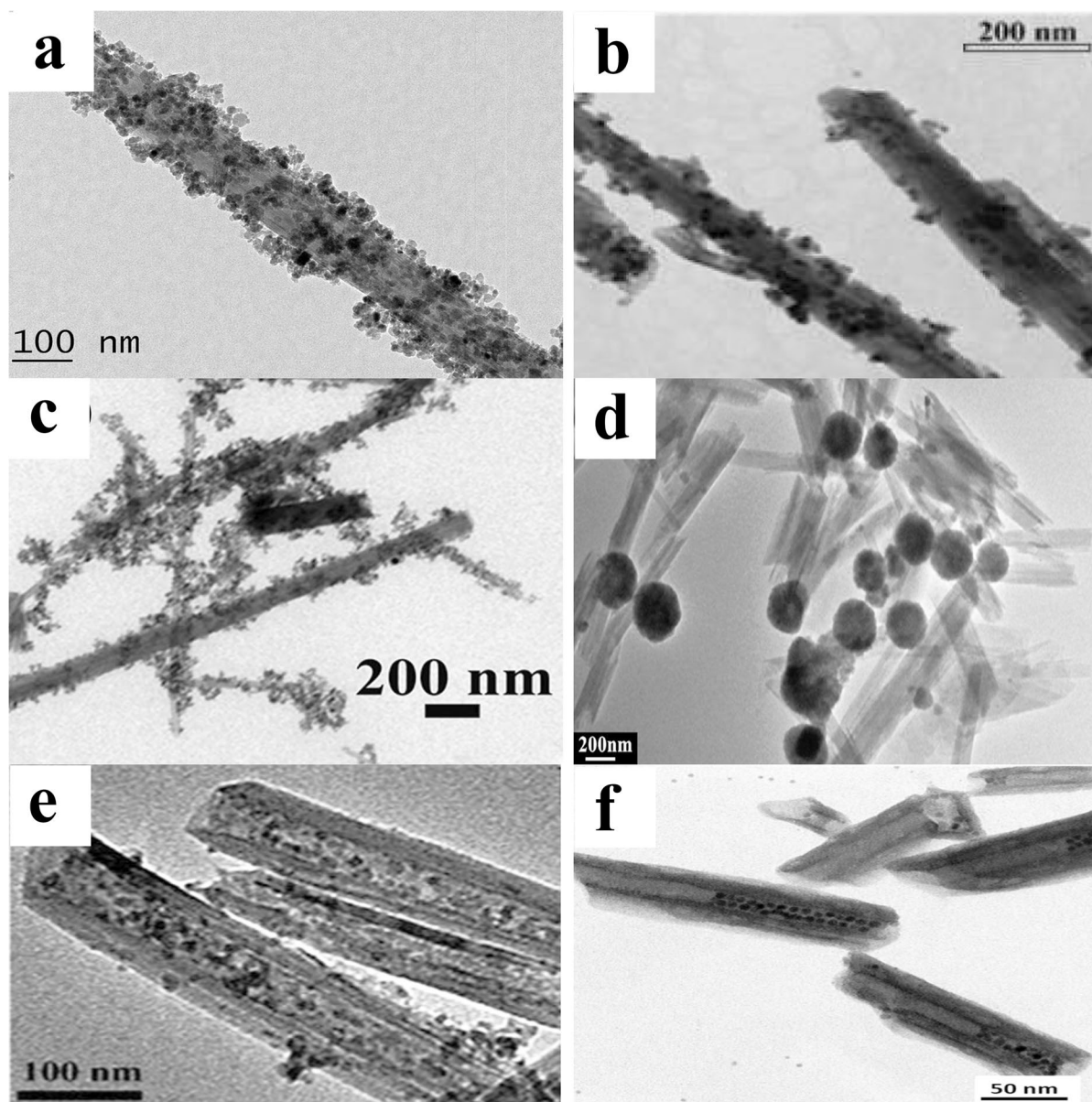


**Fig. 5** TEM images of MHNTs prepared by: **a** co-precipitation (reproduced from Fizir et al. (2017); Li et al. (2018a) with the permission of Elsevier), **b, d** solvothermal (reproduced from Pan et al. (2011) with permission of the American Chemical Society), **c** direct mixing (reproduced from Mu et al., 2014b with permission of Springer), **e** wet impregnation (reproduced from Pan et al., (2012a) with the permission of Elsevier), and **f** encapsulation methods (reproduced from Hamza et al. (2020) with the permission of the American Chemical Society)

10 nm (Fig. 5e) (Pan et al., 2012a). As for the morphology of MHNTs synthesized by the encapsulation method, functionalized MNPs of diameter  $\sim 6$  nm were loaded in their entirety into the lumens of HNTs (Fig. 5f) (Hamza et al., 2020).

### Surface Functional Modification of MHNTs

When MHNTs are used as adsorbents for pollutants or other analytes, MHNTs show only a weak affinity (ion exchange, hydrogen bonding, and van der Waals forces)

for the guest. To enhance the performance of MHNTs in the above-mentioned area, surface functionalization of MHNTs (Fig. 6), normally site-specific and sometimes selective, is extremely advantageous.

#### Functionalization of MHNTs-Based Silane Coupling Agent

Modification of inorganic nanomaterials using a silane agent is a chemical surface modification approach that has attracted much interest to control dispersion and aggregation of nanoparticles (Ahangaran & Navarchian, 2020). Silane modifiers are one of the most significant bifunctional modifiers that are used commonly for the surface functionalization of HNTs or MHNTs (Fig. 7). The most important characteristic of silane modifiers (Table 4) is their capability to create a stable chemical bond between organic and inorganic MHNTs. Typically, silane coupling agents are grafted on MHNTs via covalent modification. The reaction mechanism of the grafting process is the condensation between the hydrolyzed silanes and the hydroxyl groups located on the external surfaces of the MHNTs (Liu et al., 2014). External

surface modification can improve the adsorption efficiency of MHNTs (Zhu et al., 2017) and is considered as a vital step to prepare polymer composites because silane coupling improves the bonding performance of organic polymers (Foroughirad et al., 2020a; Hajizadeh & Maleki, 2018; Zhu et al., 2020). Generally, dispersions of the MHNTs and silane agents may undergo condensation reactions in toluene (Kadam et al., 2017), acetic acid/alcohol (Sillu & Agnihotri, 2019), water/alcohol (Hang et al., 2013), or ethyl alcohol (Zhu et al., 2017). All reactions were kept under reflux conditions (60°C) for 24 h or more. MHNTs may also be modified by 3-amino-npropyltriethoxysilane (APTES), through which the ending amine group is anchored onto the MHNT's surface to initiate the polymerization process (Foroughirad et al., 2020a). Reportedly, the uniform silanol (Si–OH) sites over MHNTs can be transformed into much stronger siloxane (Si–O–Si) bonds through amino silanization by APTES, causing orientation of amine groups away from the surface (Sillu & Agnihotri, 2019).

Recently, surface vinyl functionalization of the MHNTs by methacryloxy propyl trimethoxyl silane was developed to introduce polymerizable double

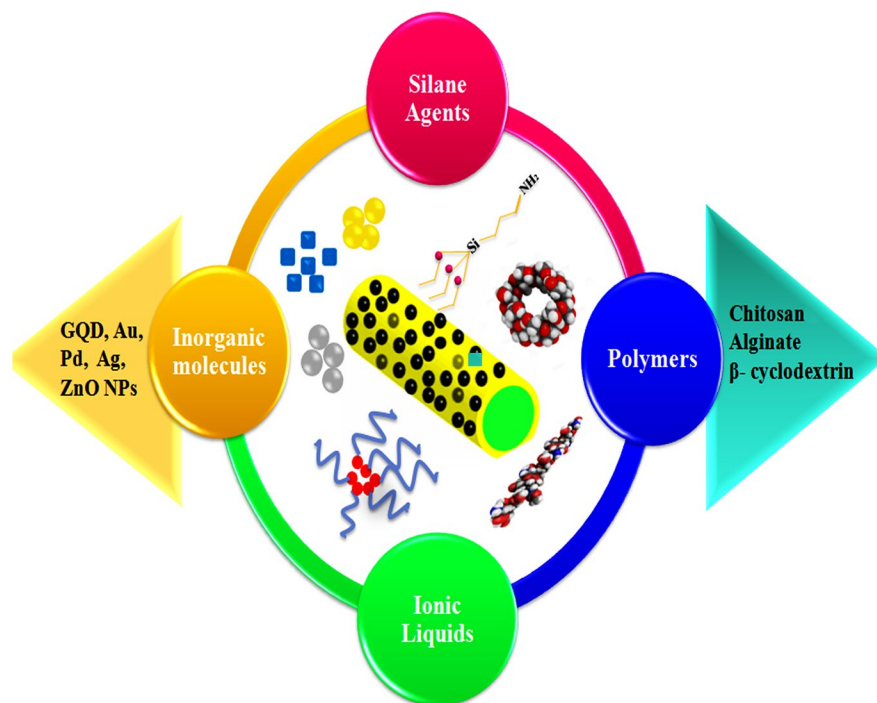


**Fig. 6** Surface functional modification of MHNTs with various organic and inorganic molecules

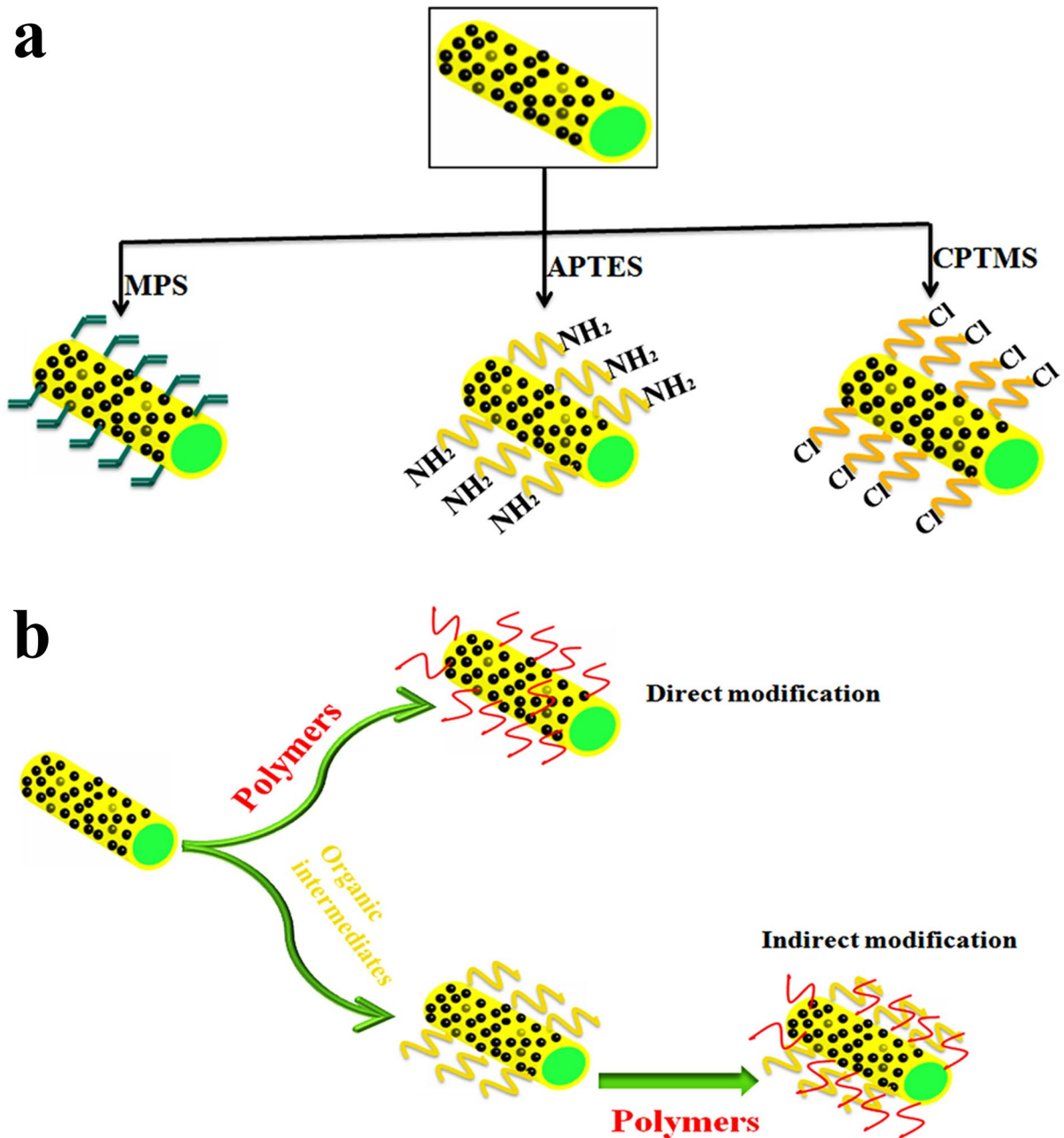


**Fig. 7** **a** Functionalization of MHNT-based silane coupling agents and **b** polymer modification approaches

bonds (Fizir et al., 2018b). Thermogravimetric analysis (TGA) showed that the grafting ratio was 9.60% (relative to MHNTs) (Hang et al., 2013; Sun et al., 2016). Silane coupling agents including anilino-methyl-triethoxysilane and 3-piperazinepropylmethyl-di-methoxysilane were grafted on MHNTs to increase the adsorption capacity of magnetic

nanotubes. The grafting reaction was performed in ethyl ethanol solution. Analysis by TEM showed a thin layer of membrane coated on the surface of MHNTs. The specific surface area of the modified MHNTs decreased because the micro-pores of the HNTs were partially plugged by the silane (Zhu et al., 2017).

**Table 4** Silane coupling agents used for modification of MHNTs

Commercial name	Chemical Name	References
KH-42	Aniline-methyl-triethoxysilane (AMTS)	(Zhu et al., 2017)
KH-108	3-piperazine propyl methyl dimethoxysilane (PPMS)	(Zhu et al., 2017)
KH-590	3-Mercaptopropyl triethoxysilane (MPTS)	(Zhu et al., 2017)
KH-791	N-(3-(Tri-methoxysilyl)propyl)ethylene-diamine	(Zhu et al., 2017)
KH550	3-Amino-npropyltriethoxysilane (APTES)	(Foroughirad et al., 2021; Fu et al., 2016; Zhu et al., 2020)
KH230	3-chloropropyltriethoxysilane(CPTMS)	(Hajizadeh et al., 2020a)
KH570	Methacryloxy propyl trimethoxyl silane (MPS)	(Hang et al., 2013; Sun et al., 2016; Zhu et al., 2015)
A174	3-(trimethoxysilyl) propylmethacrylate (TMSPMA)	(Dai et al., 2014; Huang et al., 2020)

Silane grating methods can be employed further as a pretreatment before additional surface modifications. For example, to prepare MHNTs-Ag, MHNTs was modified with APTES where the amino groups of APTES were complexed with silver ions and formed large clusters on the surface of MHNTs (Fu et al., 2016). In another study, to synthesize MHNTs-COOH, MHNTs were first functionalized with amino groups by grating APTES. Subsequently, the MHNTs-NH<sub>2</sub> product was mixed and stirred with succinic anhydride in dimethyl formamide, generating the MHNTs-COOH (Pan et al., 2012a).

#### Functionalization-based Polymers

The preparation of MHNTs with high sorption efficiency has recently become a new research hotspot. The MNPs introduced on magnetic nanotube surfaces cause adverse defects such as lower uptake capacity, which restricts their large-scale application, however. Fortunately, the aforementioned drawback has been solved successfully via the selective modification of MHNTs with natural and synthetic polymers (Yang et al., 2013a). As expected, the nano-composites obtained exhibited outstanding utility in the removal of heavy metal ions, dyes, and organic contaminants. The functionalization of MHNTs with the polymer layer increases not only the binding capacity but also the mechanical and thermal stability, thereby resulting in an adsorbent with superior properties compared to those of either the magnetic nanotubes themselves or the polymer (Khunová et al., 2016; Liu et al., 2014; Vahidhabanu et al., 2019). The external and internal surfaces of MHNTs are both polar due to the silica and alumina species which provide

sufficient hydrophilicity, and, consequently, good dispersion in polymers such as polyethyleneimine (PEI) (Hajizadeh & Maleki, 2018; Zhou et al., 2016), polyacrylates (Foroughirad et al., 2020b), and biopolymers such as chitosan (CS) (Dramou et al., 2018; Kadam et al., 2018; Kim et al., 2018; Lee et al., 2019; Vahidhabanu et al., 2019), alginate (Polat & Açık, 2019), and cyclodextrin ( $\beta$ -CD) (Li et al., 2019; Yang et al., 2013a).

Many publications exist on the functionalization of MHNTs with chitosan (Dramou et al., 2018; Kadam et al., 2018; Kim et al., 2018; Lee et al., 2019; Vahidhabanu et al., 2019). The hybridization is achieved by simple solution mixing of MHNTs with CS solution in a suitable solvent with vigorous stirring or ultrasonic treatment in the presence of glutaraldehyde as a cross-linker (Kadam et al., 2020a; Türkeş & Açık, 2020). MHNTs can interact with cationic polymers, such as CS and PEI, via electrostatic attraction (Kadam et al., 2020b). MHNTs were modified with chitosan oligosaccharides (COS) via a simple assembling method with a 5.9% grafting ratio. The cationic amine group of COS interacts with the negatively charged outer surface of MHNTs through electrostatic attraction. Moreover, the Si-O groups of MHNTs can interact with the amine and hydroxyl groups of chitosan oligosaccharides via hydrogen bonding (Dramou et al., 2018).

Water-soluble polymers such as PEI can also be mixed directly with magnetic halloysite. In a study by Zhu et al. (2020), branched PEI with sufficient amino groups was used to cross-link to MHNTs-APTES using glutaraldehyde. PEI has shown effective binding with MHNTs; its intrinsic toxicity problem needs to be addressed, however. MHNT-alginate

nanocomposite gel beads can be prepared by mixing the MHNTs in water and crosslinking them using calcium ions (Polat & Açıkel, 2019).

In measurement with MHNT-polymer composites, MHNTs can be modified by cyclodextrin via covalent functionalization where amide bonds are formed between carboxylated  $\beta$ -CD and the primary amines on MHNTs (Li et al., 2019).

Apart from being used to prepare MHNT-polymer nanocomposites, these interactions can also be employed for the surface treatment of MHNTs for further modification such as enzyme immobilization for catalytic purposes (Kadamet al., 2020b; Zhu et al., 2020). Note that enzyme immobilization can also be carried out without polymer modification as reported by Sillu and Agnihotri. (2019), in which cellulase was immobilized directly on the amine-modified MHNTs using aminosilane surface functional chemistry.

MHNTs have also been used as support to initiate surface polymerization of various kinds of monomers such as methacrylic acid, acrylamide, acrylic acid, etc. For example, novel MHNTs grafted polymer using vinyl monomers has been prepared for a sustained-release drug-delivery system (Fizir et al., 2017). Similarly, [2-(acryloyloxy) ethyl]trimethylammonium chloride (AETAC) along with APTES has been used as monomers and grafted on the surface of MHNTs via co-precipitation polymerization (Foroughirad et al., 2020b).

From the studies above, polymer functionalization of MHNTs can be achieved by direct or indirect approaches. Direct polymer functionalization is carried out directly on the surface of MHNTs whereas, indirect functionalization is achieved by surface modification of MHNTs with organic intermediates (bridge) such as APTES or glutaraldehyde to adjust the compatibility between the inorganic cores (MHNTs) and the polymer shell. Despite the direct method being simple, the indirect method is the more convenient pathway and leads to a higher graft ratio of polymer (Gao, 2019). Polymer modification approaches are simplified and depicted in Fig. 7b.

#### Functionalization-based Inorganic Materials

Anchoring small inorganic molecules such as graphene quantum dots (GQD), gold (Au) (Jia et al., 2016), palladium (Pd) (Jia et al., 2017), silver (Ag) (Gan et al., 2015; Rouhi et al., 2020), and zinc oxide

(ZnO) NPs (Jee et al., 2020), etc., on the surface of MHNTs is the easiest functionalization approach. There are two strategies of modification. The first consists of adding one, two, or more small inorganic molecular materials into a solution containing magnetic HNTs. The small inorganic molecules interact with each other and condense on the surface of MHNTs. As proof of concept, MHNTs have been modified successfully with inorganic antimicrobial zinc oxide (ZnO) NPs in two steps: first, the  $Zn^{2+}$  ions were attached tightly to the negative surface of the MHNTs; and second, the calcination treatment led to the nucleation of  $Zn^{2+}$  to form the ZnO on the surface MHNTs (Jee et al., 2020).

Ag nanoparticles with a mean diameter of 20 nm were embedded on the external surfaces of MHNTs via the chemical-reduction method where  $AgNO_3$  was used as a precursor and mixed with a MHNTs dispersion. The TEM results showed that Ag NPs were spherical in shape (Gan et al., 2015). MHNT-AuPd was synthesized by mixing MHNT solution with the NPs precursor's solution ( $HAuCl_4$  and  $K_2PdCl_4$ ) at ambient temperature. The TEM results showed that AuPd NPs with diameters of  $<5$  nm were formed and deposited on the surface of MHNTs (Jia et al., 2017).

The second strategy consists of immobilization or self-assembly of the inorganic metal compound directly on the surface of the magnetic HNTs. This strategy was exploited to prepare MHNT-Au and MHNT-Au-Ni where Au or Au-Ni NPs arranged on the external wall of MHNTs by simply blending the Au or Au-Ni NPs with thiol-group-modified MHNTs via metal-S bonds (Jia et al., 2016). The outer surfaces of APTES-modified MHNTs was decorated with AuNPs via electrostatic interaction (Fig. 8) (Zhang et al., 2020).

Similarly, a graphene quantum dot with excellent electrical properties was anchored on the external surface of MHNTs through covalent immobilization. The GQD/MHNTs can be synthesized by thermal decomposition of citric acid to produce GQD and subsequently form amide bonds between carboxylated GQD and amine-modified MHNTs via the EDC/NHS reaction (Zare Pirhaji et al., 2020a; Zare Pirhaji et al., 2020a, 2020b). The same strategy was used to prepare functionalized MHNTs with N-doped graphene quantum dots (Ganganboina et al., 2017). The uniform dispersion of GQD with a mean diameter of 7 nm on the MHNT surfaces was confirmed by

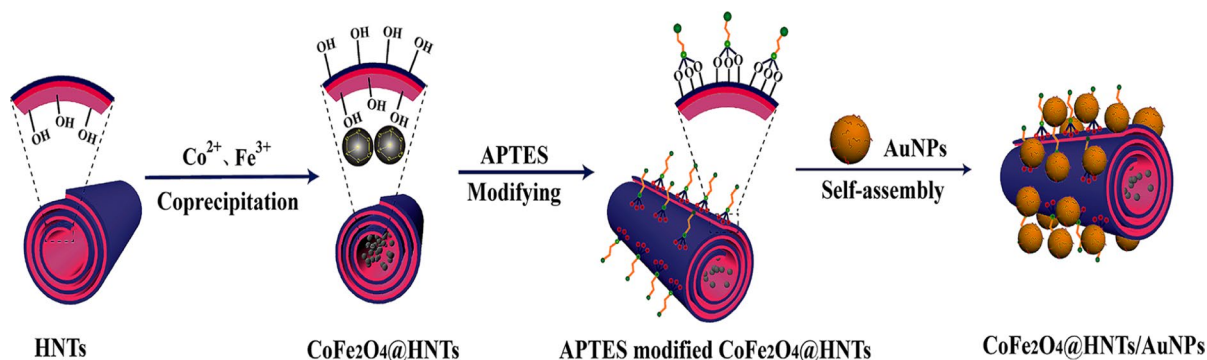


**Fig. 8** Synthesis process of MHNT/AuNP composites (reproduced from Zhang et al. (2020) with the permission of the American Chemical Society)

TEM analysis. The nanocomposites (NiFe<sub>2</sub>O<sub>4</sub>/HNTs/GQDs) prepared showed significant superparamagnetic features (60.82 emu g<sup>-1</sup>).

#### Functionalization-based Ionic Liquids

Ionic liquids (ILs), defined as low melting-point organic salts, are a novel class of compounds with unique properties and a combinatorially broad chemical diversity (Ghandi, 2014). The surface functionalization of nanoparticles by ionic liquids attracts significant research attention. Ionic liquids such as cetyltrimethyl ammonium bromide (CTAB), sodium dodecyl sulfate (SDS), or 1-hexadecyl-3-methylimidazolium bromide (C<sub>16</sub>mimBr) were adsorbed on the surfaces of various nanomaterials such as CNTs (Bai et al., 2011), GO (Das et al., 2013), and HNTs (Abhinayaa et al., 2019) to enhance their stability and loading capacity. More recently, C<sub>16</sub>mimBr has been coated, in non-covalent fashion, on the surfaces of MHNTs by means of a simple sonication treatment. The formation mechanism consists mainly of electrostatic interaction between the C<sub>16</sub>mim<sup>+</sup> and negatively charged MHNTs. The formation of C<sub>16</sub>mimBr with mixed hemimicelles on the surfaces of MHNTs led to the retention of analytes by strong hydrophobic,  $\pi$ - $\pi$ , and electrostatic interactions which led to an increase in the uptake capacity of the MHNTs (Liu, et al., 2018a). Based on the encouraging results obtained from the nanomaterials above, novel mixed hemimicelles on the surfaces of MHNTs have been developed using two types of

ionic surfactants (non-ionic surfactant (TX100) and 1-cetyl-3-methylimidazolium bromide (C<sub>16</sub>mimBr)) to endow the mixed hemimicelles with more hydrophobic properties. The ratio of TX100/C<sub>16</sub>mimBr 0.64 showed significant recovery of the extracted analytes whereas increasing the amount of TX100 resulted in a poor extraction rate due to the saturation of the MHNT-C<sub>16</sub>mimBr (Liu et al., 2018b). The analytical achievement of the above-functionalized MHNTs will be discussed in the next section.

#### Analytical and Environmental Applications of MHNTs and MHNT Nanocomposites as Magnetic Adsorbents

The removal of emerging contaminants, e.g. dyes, heavy metal ions, radioactive ions, pesticides, etc., by adsorption, offers numerous advantages such as low cost, biocompatibility, and removal efficiency over other cleanup methods. The key player in applying MHNT nanocomposites as adsorbents is a special tubular structure that does not exist in other nanomaterials and is ideally suited to the task of contaminant destruction and elimination. MHNT nanocomposites are not limited to separation of contaminants from environmental wastewaters; they can also be used in monitoring and detection of various therapeutic agents, proteins, and mycotoxins in biological and food samples. The analytical application of MHNTs has gained significant attention (Fig. 9) where the removal of dyes and heavy metal ions is the main requirement.



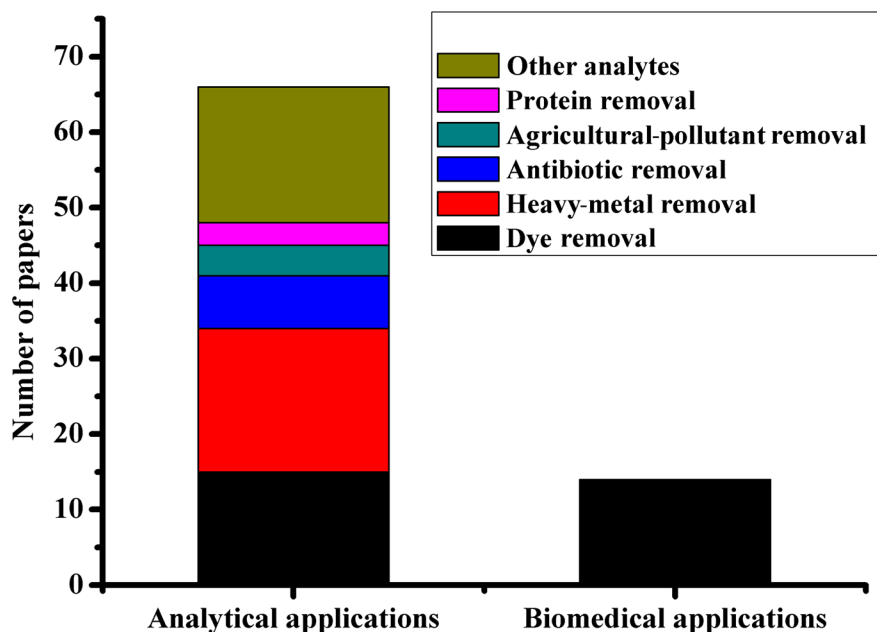


**Fig. 9** Number of papers published relating to fields of application of MHNTs and various adsorbed analytes

#### MHNTs and MHNT Nanocomposites for Dye Removal

Wastewaters containing dyes are hazardous and carcinogenic to human beings (Zhou et al., 2019). Various researchers have attempted to develop substitute nanomaterials for dye adsorption. In this section, the dye adsorption and removal capability from aqueous and environmental samples of MHNTs and composites-based MHNTs is compiled. The adsorption of dyes by MHNTs was investigated first by Xie et al. (2011). MHNTs exhibited better adsorption of cationic methylene blue (MB) than neutral red (NR) and methyl orange (MO). However, the adsorption capacity of HNTs was twice as great as that of MHNTs. The comparable results between the three dyes studied are due to the negatively charged surfaces of MHNTs which could adsorb more cationic dyes such as MB (Xie et al., 2011). In another work, MHNTs showed a maximum adsorption capacity of  $11.10 \text{ mg g}^{-1}$  for  $100 \text{ mg L}^{-1}$  naphthalene green (Riahi-Madvaar et al., 2017). An increase in the MB adsorption capacity of  $57.13 \text{ mg g}^{-1}$  was observed using HNT/Fe<sub>3</sub>O<sub>4</sub>/C as an adsorbent (Jiang et al., 2014a).

In measurements involving dye removal, the mechanical strength of supramolecular gels was

improved by introducing MHNTs in their structures and it is used for dye adsorption. However, the resulting adsorption capacity was very small (Zeng et al., 2016) and was similar to unmodified MHNTs (Xie et al., 2011). Consequently, this multistep-prepared supramolecular gel is not recommended for dye adsorption. MHNTs were functionalized by various kinds of polymers (i.e. polydopamine and chitosan) and ionic liquids to enhance their dye-adsorption capacity. An excellent MB-removal capacity, up to  $714.29 \text{ mg g}^{-1}$ , was obtained using the core-double-shell structured MHNTs/poly(dopamine + APTES) nano-hybrids as adsorbents. The removal efficiency reached 89% for MB after five adsorption–desorption cycles, which means that the nanohybrids possess an outstanding regeneration capacity. The excellent removal efficiency is attributed to the fact that MHNTs/poly(dopamine + APTES) possessed a large number of negatively charged amine groups and catechol groups under an alkaline medium, which could react with MB through the electrostatic interaction and  $\pi$ – $\pi$  stacking interaction (Wan et al., 2017). The aforementioned material was used in the polyvinylidene fluoride (PVDF) membrane to enhance its hydrophilicity and water flux. These composites showed a good MB removal rate of  $\sim 97.2\%$  (Zhang et al., 2019).

Similarly, 2-(acryloyloxy)ethyl-trimethylammonium chloride (AETAC) and APTES as cationic and co-monomers, respectively, were polymerized on the surface of MHNTs and used as adsorbents of sunset yellow. The composites showed a large and quick adsorption capacity of  $33.8 \mu\text{mol g}^{-1}$  in only 15 min. The dominant adsorption mechanism was the electrostatic interactions between the anionic sulfonic acid groups of the dye and the cationic functional groups of the monomer AETAC (Foroughirad et al., 2020b).

More recently, chitosan-modified MHNTs as adsorbents for dye removal have attracted significant research attention. For example, sponge-like MHNT/CS composite synthesized by combining solution-mixing and freeze-drying showed a maximum Congo red dye adsorption capacity of  $54.49 \text{ mg g}^{-1}$ , which was greater than that of HNTs/CS ( $41.54 \text{ mg g}^{-1}$ ) due to the additional surface charge provided by MNPs. Electrostatic interactions play an important role in the binding between dye and MHNTs/CS (Vahidhabanu et al., 2019). The aforementioned adsorbent also showed a good MB adsorption ability of  $50.37 \text{ mg g}^{-1}$  (Türkeş & Açikel, 2020).

The uptake capacity of MO has been improved by using mixed hemimicelles-based MHNTs as low-cost adsorbents. The outcomes indicate that MHNTs- $\text{C}_{16}\text{mimBr}$  could adsorb  $\sim 150 \text{ mg}$  of MO and  $90 \text{ mg}$  of methyl red (MR) per gram of MHNTs. This good adsorption efficiency may be due to the following: (1) dyes could interact with adsorbents through electrostatic,  $\pi$ - $\pi$ , and hydrophobic interactions provided by the micelles adsorbed on the surfaces of MHNTs; and (2) the lumen of HNTs could retain the dyes through the electrostatic interaction between  $\text{OH}^{2+}$  of the aluminum group (Al-OH) and negative charge of MO and MR. This adsorbent showed significant rates of recovery, 85–87% for MR and 89–93% for MO from tap and lake waters, and low detection limits,  $0.042 \mu\text{g L}^{-1}$  for MR and  $0.050 \mu\text{g L}^{-1}$  for MO (Liu et al., 2018a).

The reviewed literature shows that polydopamine-grafted MHNTs and MHNTs- $\text{C}_{16}\text{mimBr}$  are the best substitute nanomaterials for MB and MO removal from environmental wastewaters, respectively. However, further research is needed for the application of polydopamine-grafted MHNTs in real samples. In addition, the selectivity of the aforementioned materials should be enhanced by grafting new elements on the surfaces of MHNT-based

composites. The application of MHNT nanocomposites to different kinds of dyes is summarized in Table 5.

#### MHNTs and MHNTs Nanocomposites for Heavy Metal Removal

Heavy metal ions pose a tremendous threat to ecosystems and living creatures due to their high toxicity (Siddeeg et al., 2021). MHNT nanocomposite materials have a special macro and mesoporous structure and excellent adsorption performance which can be applied to adsorption and removal of heavy metal ions. In this section, the role and potential of MHNTs in heavy-metal ion elimination from real samples will be reviewed.

#### Monovalent Heavy Metal Ions

Magnetic HNTs were employed as adsorbents to study the adsorption characteristics of some monovalent metal ions such as Ag(I) and Tl(I). The quantification of these metal ions using MHNTs will be summarized in this section.

Thallium (Tl) is among the most significant toxic metal ions in drinking water. However, it has been studied only rarely (Shah et al., 2019). A new nanocomposite consisting of magnetite halloysite nanotubes and dibenzo-18-crown-6 was developed for the preconcentration of Tl(I) via ultrasound-assisted solid-phase extraction combined with electrothermal atomic absorption spectrometry. Dibenzo-18-crown-6 was used due to its selectivity for Tl(I) ions. The methods demonstrated significant recovery of Tl(I) from real samples such as tap water and human hair, up to 104% and the detection limit was  $1.8 \text{ ng L}^{-1}$  (Ashrafzadeh Afshar et al., 2017).

Magnetic halloysite nanotubes modified with 5-(p-dimethylaminobenzylidene) rhodanine, a silver-specific dye, has been investigated as a selective adsorbent for the removal of Ag(I) from environmental samples. The adsorbent possessed a fast adsorption capacity of  $16.2 \text{ mg g}^{-1}$  in 45 min. In the concentration range from  $4.0$  to  $200 \mu\text{g L}^{-1}$  of  $\text{Ag}^+$ , the limit of detection was  $1.6 \mu\text{g L}^{-1}$ . The recovery of silver ions from the soil sample was up to 102.0% and no interferences were detected (Amjadi et al., 2015a).

**Table 5** Summary of the application of MHNT nanocomposites to various kinds of dyes

MHNT nanocomposites	Dyes	Experimental conditions			Adsorption capacity (mg g <sup>-1</sup> )	LOD (µg L <sup>-1</sup> )	References
		Concentration (mg L <sup>-1</sup> )	pH	T (°C)			
MHNTs	Methylene Blue	37.4	7	25	18.49	–	(Xie et al., 2011)
	Methyl Orange	32.7			<2		
	Neutral Red	28.9			13.62		
MHNTs	Naphthalene Green	100	3	25	11.10	–	(Riahi-Madvaar et al., 2017)
HNT/Fe <sub>3</sub> O <sub>4</sub> /C	Methylene Blue	70	7	25	57.13	–	(Jiang et al., 2014a)
Supramolecular gels	Congo Red	–	–	–	9		(Zeng et al., 2016)
	Methyl Orange				2		
	Malachite Green				1.2		
MHNTs/ poly(dopamine + APTES)	Methylene Blue	70	10–11	45	714.29	–	(Wan et al., 2017)
MHNTs/ poly(dopamine + APTES)/ polyvinylidene fluoride	Methylene Blue						(Zhang et al., 2019)
AETAC-APTES/MHNTs	Sunset Yellow	4.39 <sup>a</sup>	2	25	33.8 <sup>c</sup>	–	(Foroughirad et al., 2020b)
MHNT/Chitosan	Methylene Blue	200	11	25	50.37	–	(Türkeş & Açık, 2020)
	Congo Red	200	7	30	41.54	–	(Vahidhabanu et al., 2019)
MHNTs-C <sub>16</sub> mimBr	Methyl Orange	50.10 <sup>-6</sup>	7.5	25	150	0.050 <sup>*</sup>	(Fizir et al., 2018a)
	Methyl Red				90	0.042 <sup>*</sup>	
MHNTs-MIP	Sunset Yellow	43 <sup>b</sup>	2	30	46.4 <sup>c</sup>	–	(Foroughirad et al., 2021)

<sup>a</sup>µM/mL, <sup>b</sup>µmol/L, and <sup>c</sup>µmol/g

\* Detection technique: HPLC–UV

## Divalent Heavy Metal Ions

Several types of divalent metal ions such as Cu(II), Pb(II), Cd(II), and Hg(II) have been adsorbed by MHNTs. The adsorption capacity of MHNTs for cadmium (Cd<sup>2+</sup>) in aqueous solution was 11.4 mg g<sup>-1</sup> and the recovery in spiked waters, nail, and hair samples by MHNTs coupled with a flame atomic absorption spectrometry method ranged from 96.7 to 104.2% with a detection limit of 0.27 µg L<sup>-1</sup> (Amjadi et al., 2015a). These results are comparable to other nanomaterials studied such as functionalized magnetic CNTs (Taghizadeh et al., 2014) and MOFs (Sohrabi et al., 2013) where they showed excellent adsorption performances (>185 mg g<sup>-1</sup>) and low detection limits (<0.20 µg L<sup>-1</sup>). However, low-cost MHNTs without functionalization still showed acceptable results for Cd<sup>2+</sup> removal and analysis whereas the other nanomaterials need labor-intensive preparation steps. In an attempt to enhance the removal capacity of MHNTs, GQD was immobilized onto the external surface of MHNTs to remove Cd<sup>2+</sup> and Pb<sup>2+</sup> from water. The adsorbent showed an improved uptake capacity of 34.72 and 42.02 mg g<sup>-1</sup> in <60 min. The

removal of metal ions is based on the construction of complexes (bidentate and monodentate) between the carboxyl and hydroxyl species on the surfaces of MHNTs/GQDs and the metal ions (Zare Pirhaji et al., 2020a, 2020b). Polyethyleneoxide/chitosan (PEO/CS) nanofibers were used to immobilize MNPs and HNTs via electrospinning. The nanofibrous adsorbents possessed a maximum adsorption capacity of ~120, 160, and 150 mg g<sup>-1</sup> under an initial concentration of 100 mg L<sup>-1</sup> at 45°C for Cd(II), Pb(II), and Cu(II), respectively (Li et al., 2018b).

Several research projects reported the elimination of Pb<sup>2+</sup> from wastewaters (Alguacil et al., 2018; Nonkumwong et al., 2016). This metal ion belongs to the hazardous heavy metal class. Pb<sup>2+</sup> is very stable in nature and if its concentration in the body exceeds 0.1 mg L<sup>-1</sup>, it can cause anemia and damage the nervous system. MHNT-manganese oxides (MHNTs-MnO<sub>2</sub>) were applied successfully to the rapid removal of Pb<sup>2+</sup> from an aqueous solution. MnO<sub>2</sub> was used due to its greater affinity for many heavy metal ions. The uptake capacity of Pb<sup>2+</sup> by MHNTs-MnO<sub>2</sub> (~60 mg g<sup>-1</sup>) was about three times greater than that of MHNTs (~20 mg g<sup>-1</sup>) (Afzali & Fayazi, 2016).

In other research, polyamide-amine (PAMAM) has been loaded on the surfaces of MHNTs to provide a large amine-group density. The maximum adsorption capacity of this material for Pb(II) was up to 194.4 mg g<sup>-1</sup>. After six cycles, MHNTs-PAMAM still retained 90% of the maximum adsorption capacity. The adsorption mechanism consists of the coordination between the internal tertiary amines and the sulfhydryl groups with the Pb cation and, when pH > 4, the adsorption capacity increased due to the reducing species of H<sub>3</sub>O<sup>+</sup> in water (Cheng et al., 2019). Similarly, MHNTs-alginate beads with a 1:2 ratio possess a large adsorption capacity for Pb(II) which was up to 125 mg g<sup>-1</sup> (Polat & Açıkel, 2019).

Mercury (Hg<sup>2+</sup>) is one of the most widely studied pollutants and its discovery in environmental samples is attracting significant research attention. Exposure to Hg<sup>2+</sup> can damage the central nervous system and vital body organs (Selvaraj et al., 2021). A simple magnetic electrochemical sensing protocol using MHNTs-MnO<sub>2</sub> and magnetic carbon paste electrodes where the Hg<sup>2+</sup> can be absorbed by MHNT composites was reported by Fayazi et al. (2016). The MHNTs composites-Hg<sup>2+</sup> was brought to the surface of the electrode where the ions are detected electrochemically by applying differential pulse voltammetry. The recovery of metal ions from real water samples was up to 102.7%. In the concentration range 0.5–150 µg L<sup>-1</sup> Hg(II), the detection limit was very small, 0.2 µg L<sup>-1</sup>. The results were comparable to other previously modified electrochemical methods such as carbon paste electrode modified magnetic nickel zinc ferrite nanocomposites (8.0 µg L<sup>-1</sup>) (Afkhami et al., 2015) and glassy carbon electrode modified ion imprinted polymeric-carbon nanotubes (1 µg L<sup>-1</sup>) (Rajabi et al., 2013).

### Variable-Valence Heavy Metal Ions

For the environmental samples mentioned above, the variable-valence heavy metal ions adsorbed by MHNT nanocomposites are chromium (Cr(III) and Cr(VI)), antimony (Sb(V) and Sb(III)), and arsenic (As(III) and As(V)).

Exposure of the human body to a low level of arsenic (i.e. drinking water containing As) can lead to serious health problems such as chronic poisoning and cancer because arsenic can combine with sulfhydryl groups and hydroxyl groups in the molecular

structure of enzyme proteins and thus affect directly the body's physiological function (Jomova et al., 2011). Magnetic HNTs showed a high adsorption capacity of 408.71 and 427.72 mg g<sup>-1</sup> for As(III) and As(V), respectively (Song et al., 2019). The elimination pathways of As are attributed to the inner-sphere complex formation and As(V) reduction with simultaneous Fe(II) oxidation (Maziarz et al., 2019).

A porous adsorbent with HNTs, Fe<sub>3</sub>O<sub>4</sub>, and carbon was produced to enhance the removal efficiency of arsenic by using polyurethane foam waste as the carbon source and structure template for HNTs dispersing and MNPs loading. The adsorbent showed an excellent uptake capacity of 1491.72 mg g<sup>-1</sup> toward As(V) due to the porous structure of HNTs/C/Fe<sub>3</sub>O<sub>4</sub> and the good dispersion of HNTs and iron oxide, which facilitate the transmitting of arsenic ions and provide more binding sites (Song et al., 2021).

The permitted level of Cr(VI) in environmental wastewaters is limited to 200 µg L<sup>-1</sup> due to its potential carcinogenicity (Tian et al., 2016; Zhitkovich, 2011). Cr(VI) is more harmful to the environment than Cr(III). Typically, the removal of this toxic element consists of reducing the most toxic Cr(VI) species and immobilizing the resulting low-toxicity Cr(III) moieties (Xia et al., 2019). For example, oxygen-containing organic groups and iron oxide nanoparticles were coated on the surface of HNTs for the removal of Cr(VI). The Fe<sub>3</sub>O<sub>4</sub>/HNTs-C produced exhibited a maximum adsorption capacity of 132 mg g<sup>-1</sup>, which is ~100 times greater than that of HNTs alone (<10 mg g<sup>-1</sup>). The adsorption mechanism was explained as follows: (1) MNPs and organic carbon species reduce part of the Cr(VI); (2) the resulting Cr(III) can be attracted to the adsorbent surface by electrostatic attraction and anchored on the surface of halloysite by the chelation effect of organic functional groups (i.e. carboxyl, aldehyde, and hydroxyl); and (3) the remaining negatively charged Cr(VI) ions could be attached to the positively charged surface of adsorbent by electrostatic attraction and ion exchange (Tian et al., 2016).

Silane-modified MHNTs were also reported as having an acceptable uptake capacity for Cr(VI) in an aqueous solution which was up to 59.90 mg g<sup>-1</sup> (Table 6) (Zhu et al., 2017). However, the removal ability of this adsorbent was smaller than those found for Fe<sub>3</sub>O<sub>4</sub>/HNTs-C (Tian et al., 2016) and electrospun membrane-based MHNTs (77.10 mg g<sup>-1</sup>) (Li et al., 2018b).

**Table 6** Summary of the application of MHNT nanocomposites to various heavy metal ions

MHNT nanocomposites	Heavy metals ions	Conditions		Adsorption capacity (mg g <sup>-1</sup> )	Recovery (%)	LOD (µg L <sup>-1</sup> )	References
		Concentration (mg L <sup>-1</sup> )	pH				
MHNTs/Dibenzo-18-crown-6	Tl(I)	–	10	16.7	104	1.8 <sup>a*</sup>	(Ashrafzadeh Afshar et al., 2017)
MHNTs/5-(p dimethyl-amino-benzylidene) rhodamine	Ag(I)	–	3	16.2	102	1.6 <sup>**</sup>	(Amjadi et al., 2015a)
MHNTs	Cd(II)	25	6	11.4	96.7–104.2	0.27 <sup>**</sup>	(Amjadi et al., 2015a)
MHNTs/GQD	Cd(II)	130	5.91	34.72	–	–	(Zare Pirhaji et al., 2020a, 2020b)
Polyethylene oxide/chitosan/MHNTs	Cd(II)	800	5	120	–	–	(Li et al., 2018b)
MHNTs-MnO <sub>2</sub>	Pb(II)	400	6	59.9	–	–	(Afzali & Fayazi, 2016)
Polyamide – amine/ MHNTs	Pb(II)	180	5.6	194.4	–	–	(Cheng et al., 2019)
MHNTs-alginate	Pb(II)	500	5	274.37	–	–	(Polat & Açikel, 2019)
Polyethylene oxide/chitosan/MHNTs	Pb(II)	800	5	160	–	–	(Li et al., 2018b)
MHNTs/GQD	Pb(II)	91	5.96	42.02	–	–	(Pirhaji et al., 2020)
Polyethylene oxide/chitosan/MHNTs	Cu(II)	800	5	150	–	–	(Li et al., 2018b)
MHNTs/MnO <sub>2</sub>	Hg(II)	–	3.5	–	–	0.2 <sup>***</sup>	(Fayazi et al., 2016)
MHNTs	As (III)	300		408.71	–	–	(Song et al., 2019)
	As (V)			427.72	–	–	
HNTs/C/Fe <sub>3</sub> O <sub>4</sub>	As(III)	30	6	34.54	–	–	(Song et al., 2021)
	As (V)			1491.72	–	–	
Fe <sub>3</sub> O <sub>4</sub> /HNTs-C	Cr (VI)	200	2	132.86	–	–	(Tian et al., 2016)
Aniline-methyl-triethoxysilane-MHNTs	Cr(VI)	40	2	59.90	–	–	(Zhu et al., 2017)
Polyethylene oxide/chitosan/MHNTs	Cr(VI)	200	5	70	–	–	(Li et al., 2018b)

<sup>a</sup>ng L<sup>-1</sup>

Detection techniques: \*ETAAS; \*\*flame atomic absorption spectrometry (FAAS) and differential pulse voltammetry (DPV)

The co-adsorption feasibility of Cr(VI) and Sb(V) was tested using silane-modified MHNTs where the adsorption mechanism was explained as follows: (1) Cr(VI) ions are attached to adsorbent surfaces through anion- $\pi$ , functional-group interactions and electrostatic interaction; (2) Sb(V) can be adsorbed through Cr(VI)-O-Sb(V) interaction on the modified MHNTs surface, and (3) Cr(VI) and Sb(V) could form Cr(VI)-O-Sb(V) complexes in solution, which are subsequently adsorbed onto the adsorbent by complexation reactions. Therefore, the coexistence of Cr(VI) could enhance Sb(V) adsorption where the maximum Sb(V) adsorption capacity was found to be 30.49 and

53.06 mg g<sup>-1</sup> (Table 6) in the absence and the presence of Cr(VI), respectively (Zhu et al., 2017).

#### Application of MHNT and MHNT Nanocomposites to Radioactive Ions

The use of oil and fossil fuels leads to the pollution of water by the release of a large quantity of radioactive materials into nature. Radionuclides, such as uranium (U), are very toxic (Todorov & Ilieva, 2006). Therefore, U(VI)-bearing effluents must be treated effectively before being discharged into the environment. Adsorption of U(VI) onto MHNTs was studied

by He et al. (2015). The experimental results indicated that MHNTs had the largest adsorption capacity of  $88.32 \text{ mg g}^{-1}$  for  $\text{UO}_2^{2+}$ . The removal capacity was achieved by ion exchange and surface complexation (He et al., 2015).  $\beta$ -cyclodextrin was grafted onto MHNTs and batch adsorption techniques for U were performed (Yang et al., 2013b). The removal percentage by CD/HNT/iron oxide of uranium ions in simulated wastewater was 92% at neutral pH, showing that CD/MHNT is a promising adsorbent of uranium. The large sorption capacity of uranium was attributed mainly to the multiple hydroxyl sites of surface-grafted  $\beta$ -CD (Yang et al., 2013a). The elimination of other toxic radioactive ions, such as europium (Eu) and iodine(I) by MHNT composites warrants further research.

#### MHNT and MHNT Nanocomposites for Extraction and Detection of Pharmaceuticals, Agricultural Pollutants, Proteins, and Mycotoxins

Bioactive pollutants including pesticides and other pharmaceutically active compounds such as antibiotics are the cause of major concern. These chemicals have been blamed for contamination of freshwater and food sources, threatening water and food security. Pollution by these pollutants has hit various countries harder as a consequence of less stringent legislation on waste discharge from agricultural and pharmaceutical industries (Aylaz et al., 2021). On the other hand, therapeutic monitoring of drugs in biological fluids using a sensitive technique is necessary for controlling its efficacy in patients (Dramou et al., 2013).

Determination of any drug or contaminant in complex matrices by chromatographic or spectrophotometric methods needs sample pre-treatment to eliminate any potential interference. Currently, magnetic solid-phase extraction is a practice used commonly for sample clean-up because of its properties such as simplicity, the fact that it takes relatively little time, requires just a small amount of solvent, and is relatively cheap (Wu et al., 2021). Consequently, non-selective and selective nanocomposite-based MHNTs have been developed for the separation of various kinds of pharmaceuticals, agricultural pollutants (e.g. antibiotics, flavonoids, and pesticides), mycotoxins, and biomolecules, e.g. proteins.

#### Non-Selective Nanocomposite-based MHNTs

Several composite-based MHNTs have been tested to assess their adsorption performance for various types of analytes. For example, MHNTs appeared to have a relatively good removal capacity for tetracycline from an aqueous solution. In contrast, chitosan-modified MHNTs showed low uptake capacity (Guan et al., 2012; Ma et al., 2016b). Thus, chitosan modification is not recommended for the removal of tetracycline. In addition, the extraction of tetracycline from areal matrix by the nanomaterials above was not evaluated.

Recently, a MHNT/AuNPs substrate for rapid and efficient MSPE surface-enhanced Raman scattering (SERS) on-site detection of nitrofurantoin antibiotics in real samples was developed. MHNT was used because of its good dispersibility and rapid enrichment. The substrate exhibited excellent SERS activity and maximum extraction ability, within 5 min. The detection limit of nitrofurantoin in aquatic samples was  $0.014 \text{ mg L}^{-1}$  and the recovery was up to 116.3% (Zhang et al., 2020). In work by Dramou et al. (2022), a novel composite magnetic graphene oxide-MHNT (Fig. 10) was used for the extraction of rutin from Swanson health products due to its large adsorption uptake, up to  $50 \text{ mg g}^{-1}$ . This was greater than the uptake for either MGO or MHNTs when they were used as single adsorbents, as their dispersion characteristics could be enhanced by the composite because the introduction of MHNTs can expand the lamellar structure and reduce the aggregation of MGO efficiently. On the other hand, the MGO boosts the MHNTs adsorption capacity. The LOD (limit of detection) and LOQ (limit of quantification) of rutin using the MGO-MHNTs-HPLC method were 0.0325 and  $0.0975 \text{ } \mu\text{g mL}^{-1}$ , respectively. In fact, wastewaters or biological media are complex and contain interferences. Developing highly stable and selective adsorbents for contaminant removal and drug detection from the aforementioned samples has always been the motivation in the field of MSPE.

#### Selective Nanocomposites: MHNT-Imprinted Polymers

Molecularly imprinted polymers (MIPs) are considered to be smart polymers which have been proven an effective approach for clean-up and preconcentration

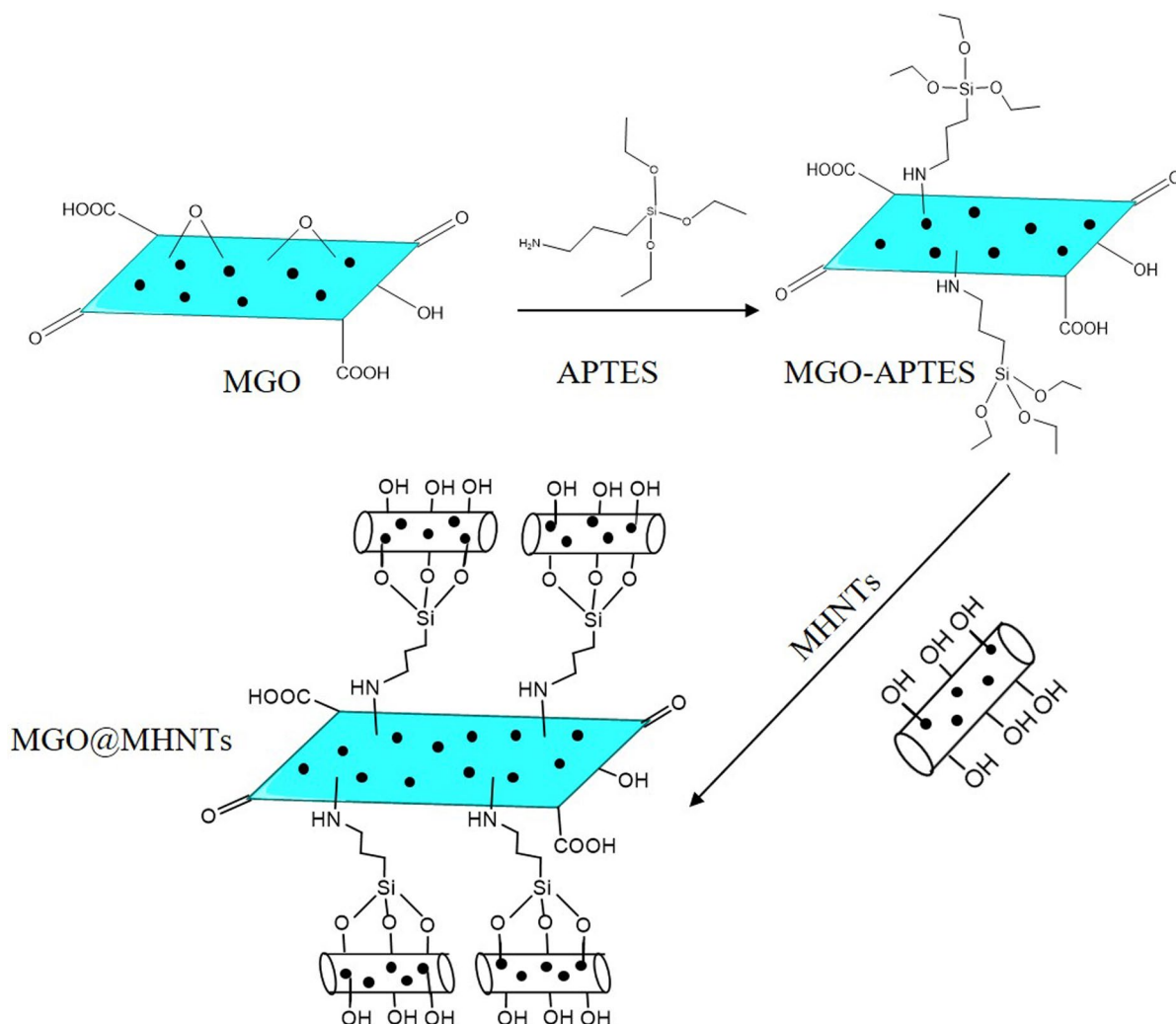


**Fig. 10** Synthesis of MGO-MHNTs (reproduced from Dramou et al. (2022) with the permission of Elsevier)

of various analytes from complex matrices (Guć et al., 2021). MIPs can uptake selectively the target molecule from a complex medium due to the recognition sites and imprinted cavity distributed in a three-dimensional network (Li et al., 2018a). To attain the recognition sites, the target analyte as the template molecule with functional monomers and crosslinker agent participates in the reaction. Based on the lock-key concept, an imprinted cavity and recognized sites were obtained after eliminating the template molecule from the designed polymer matrix, and they can select and extract the target analyte (Fizir et al., 2021).

HNTs possess superior characteristics compared to other non-support materials used such as CNTs or GO (Dramou et al., 2018). For example, modification of CNTs is necessary prior to use because they show poor dispersibility in the organic phase or aqueous phase. By contrast, HNTs disperse well in water (Fizir et al., 2020). What is more, a HNT can load molecules into its lumen which can improve the loading capacity of the MHNT composites (Fizir et al., 2020; Yamina et al., 2018). Given that HNTs possess these excellent performances, magnetic HNTs can be a good candidate and suitable alternative support or matrix for MIPs (Li et al., 2018a).

One of the most significant merits of the coating of MHNTs with MIPs (MHNTs-MIPs) is their dramatically enhanced selectivity and adsorption capacity. Many drawbacks of traditional MIPs such as poor site accessibility for templates, slow mass transfer, laborious centrifugation or filtration, and template leakage could be solved by applying MHNTs-MIPs where the separation and recovery of adsorbents are facilitated by using an external magnetic field (Fizir et al., 2020). The preparation methods of MHNTs-MIPs were discussed in a previous review (Fizir et al., 2020).

MHNTs-MIPs have been used as solid-phase extraction adsorbents for the separation of pharmaceutically active compounds, agricultural contaminants, mycotoxins, and proteins. In this section, the selectivity and adsorption capacity of these nanomaterials are discussed and highlighted.

#### Separation of Pharmaceutical Active Compounds

A series of novel selective imprinted polymer-based MHNTs was designed for the adsorption and detection of tetracycline, norfloxacin, chloramphenicol, sulfamethazine, metoclopramide, and quercetin from environmental wastewaters and biological samples, e.g. serum and urines. Methacrylic acid and EGDMA were used as a monomer and a cross-linker, respectively, to prepare MHNTs-MIPs through the co-precipitation process for tetracycline adsorption where imprinted polymers with 35 nm of shell thickness showed the greatest and fastest adsorption capacity of 21.50 mg g<sup>-1</sup> (Table 7) in 10 min due to the ultrathin imprinted polymer shell. MHNTs-MIPs showed significant stability and continuous superior performance for adsorbing tetracycline even after eight adsorption/desorption cycles (Dai et al., 2014). Reportedly, MHNTs-MIPs prepared with the template molecule and the methacrylic acid (MAA) monomer at a ratio of 1:6 exhibited an excellent selective adsorption capacity of chloramphenicol (24.44 mg g<sup>-1</sup>), excellent regeneration property, and stability. The dominant adsorption mechanism is hydrogen bonds between carboxylic acid groups of monomer and chloramphenicol (He et al., 2016a, 2016b). Ma et al. (2016a, 2016b) synthesized a novel biomimetic *Setaria viridis*-inspired-hydrophilic magnetic surface molecularly imprinted core-shell nanorods (denoted as HMMINs). Using MHNTs as carriers

enhanced significantly the specific binding of as-prepared MIPs toward sulfamethazine, 10.47 mg g<sup>-1</sup> (Table 7). However, the preparation includes many steps which are time-consuming (Ma et al. 2016a, 2016b).

With the enhancement of research on pharmaceutically active compounds, in addition to the adsorption performance of the materials in question, it is still important to have stable adsorption performance in a complex matrix. Hence, MHNTs-MIPs combined with high-performance liquid chromatography (HPLC-UV) has been applied for solid-phase extraction of norfloxacin in serum and lake water samples. Besides the excellent removal capacity and selectivity of prepared MIPs, the method provided good sensitivity (the LOD was <0.0006 µg L<sup>-1</sup> in the real samples studied) and excellent recoveries of ~83% (Fizir et al., 2018b). To simplify the imprinting process and avoid the vinyl modification of MHNTs, a sol-gel method was used to prepare MHNTs-MIPs for extraction of norfloxacin. Similar findings (to those in the research mentioned above) were made using the MHNTs-MIPs-UV method (Li et al., 2018a). Subsequently, the application of the above-produced MHNTs-MIPs was extended to the separation and detection of quercetin from serum and urine samples. APTES and TEOS were used as monomer and cross-linker agents, respectively. The MHNTs-MIPs-HPLC method showed a high sensitivity for quercetin; the limits of detection were 0.51 ng mL<sup>-1</sup> in serum and 0.23 ng mL<sup>-1</sup> in urine (Fizir et al., 2021).

MHNTs-MIPs prepared through surface-initiated reversible addition-fragmentation chain transfer polymerization could adsorb 37.8 mg of metoclopramide g<sup>-1</sup> of adsorbent with an imprinting factor of 4.51, which means that the imprinted polymers possess excellent selectivity. In the concentration range of 5.0–150.0 ng mL<sup>-1</sup> metoclopramide in urine samples, the limit of detection of MHNTs-MIPs coupled UV-Vis was calculated to be 1.5 ng mL<sup>-1</sup>. The results were comparable with other detection techniques such as HPLC, fluorescence, and UV-Vis where the LOD of the drug was >0.51 µg mL<sup>-1</sup> (Bilici et al., 2020).

In the first attempt to increase further the magnetism and loading capacity of MHNTs-MIP, it was combined with MGO via electrostatic interaction for rutin extraction. As shown in Fig. 11, strong magnetism (26.398 emu g<sup>-1</sup>), greater selectivity (IF = 2.25), and maximum adsorption capacity were obtained



**Table 7** Experimental conditions for detection and extraction of various kinds of analytes by selective and non-selective MHNT composites and their analytical performance

MHNT composites	Analytes	Concentration (mg L <sup>-1</sup> )	pH	T (° C)	Contact time (min)	Adsorption capacity (mg g <sup>-1</sup> )	Recovery (%)	LOD (µg mL <sup>-1</sup> )	References
Selective composites	Pharmaceutical active Compounds								
	Tetracycline	800 <sup>a</sup>	5	25	10	21.50	–	–	(Dai et al., 2014)
	Norfloxacin	550 <sup>b</sup>	12	25	60	312.08	85.4–96.4	0.005*	(Li et al., 2018a)
		550 <sup>b</sup>	6.9	25	250	349	83.76–103.30	0.005**	(Fizir, et al., 2018b)
	Chloramphenicol	150 <sup>a</sup>	7	45	20	24.442	–	–	(He et al., 2016a)
	Sulfamethazine	120 <sup>a</sup>	7	25	45	10.47	–	–	(Ma et al., 2016a)
	Metoclopramide	30	9	25	20	37.8	92.8–99.2	1.5 <sup>b*</sup>	(Bilici et al., 2020)
	Quercetin	100	10	25	30	169.271	95.20–103.73	0.51–0.23 <sup>b**</sup>	(Fizir et al., 2021)
	Rutin	200	7	25	120	132	90.4–94	0.27	(Wang et al., 2022)
MHNTs-MIPs	Agricultural pollutants								
	2,4,6Trichlorophenol	250	5	25	20	246.73	–	–	(Pan et al., 2011)
	2,4,5Trichlorophenol	120	6	60	12 <sup>d</sup>	197.7	–	–	(Pan et al., 2012a, 2012b)
	Dichlorophenoxyacetic acid	600	7	25	30	35.2	85–94	–	(Zhong et al., 2014)
	Lambda-cyhalothrin	300	–	25	12 <sup>d</sup>	25	–	–	(Hang et al., 2013)
	Proteins								
	Bovine hemoglobin	0.7	7	25	70	350	–	–	(Sun et al., 2016)
	Bovine serum albumin	2	7	20	80	258	–	–	(Zhu et al., 2015)
	Bovine serum albumin	500	7	25	45	48.4	–	–	(Li et al., 2020b)
	Mycotoxins								
Sterigmatocystin	150 <sup>b</sup>	5	35	40	52.08	88.62–102.91	1.1 <sup>f***</sup>	(Wang et al., 2020b)	
Zearalenone	15 <sup>c</sup>	–	25	3 <sup>d</sup>	6.38 <sup>e</sup>	74.95–88.41	2.5 <sup>b****</sup>	(Huang et al., 2020)	
Non-Selective composites									
	MHNTs	Tetracycline	40	5	35	150	34	–	–
Cs/MHNTs	Tetracycline	100	5	35	80	30	–	–	(Ma et al., 2016b)

**Table 7** (continued)

MHNT composites	Analytes	Concentration (mg L <sup>-1</sup> )	pH	T (°C)	Contact time (min)	Adsorption capacity (mg g <sup>-1</sup> )	Recovery (%)	LOD (µg mL <sup>-1</sup> )	References
MHNTs/Au	Nitrofurantoin	0.40	–	–	5	–	116.3	0.014 g#	(Zhang et al., 2020)
PAMAM-MHNTs	Heparin	30	7	45	60	7.5	–	–	(Eskandarloo et al., 2018)
MHNTs-TX100/	Amlodipin	1 <sup>b</sup>	–	25	10	–	73.8–81.2	–	(Liu et al., 2018b)
	Nimodipine						94.3–96.1	0.002** 0.001**	(Liu et al., 2018b)
MGO-MHNTs	Rutin	50	7	25	120	46.70	92.7–98.5	0.0325	(Dramou et al., 2022)

<sup>a</sup>µmol L<sup>-1</sup>, <sup>b</sup>µg mL<sup>-1</sup>, <sup>c</sup>ng mL<sup>-1</sup>, <sup>d</sup>hours, <sup>e</sup>ng/mg, <sup>f</sup>µg kg<sup>-1</sup>, <sup>g</sup>mg L<sup>-1</sup>. Detection techniques: \*UV-Vis, \*\* HPLC/UV-Vis, \*\*\*HPLC-DAD, \*\*\*\*HPLC-FLD and # Surface-enhanced Raman scattering

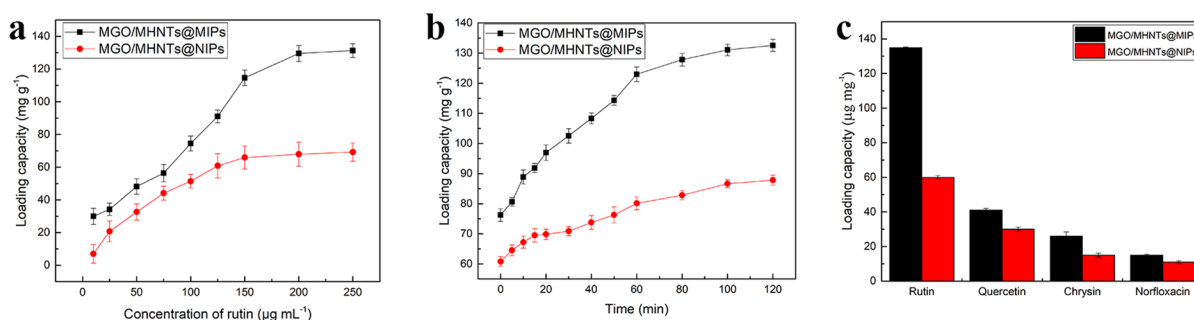


**Fig. 11** **a** The loading isotherm curve of MGO/MHNTs-MIPs and MGO/MHNTs-NIPs; **b** the kinetic loading curve of MGO/MHNTs-MIPs and MGO/MHNTs-NIPs; **c** the selectivity of MGO/MHNTs-MIPs and MGO/MHNTs-NIPs (reproduced from Wang et al. (2022) with the permission of Elsevier)

(132 mg g<sup>-1</sup>). The MGO/MHNTs-MIPs-HPLC method proved its efficiency for rutin detection and extraction from juice samples (Wang et al., 2022).

### Separation of Agricultural Pollutants

A great many pesticides, including fungicides, herbicides, and insecticides are applied in agriculture in numerous countries. These agricultural pollutants can pollute water resources with carcinogens and other toxic substances that can affect humans if they are improperly selected and managed (Mateo-Sagasta et al., 2017). MHNTs-MIPs were used as adsorbents for the removal of these pollutants, e.g. trichlorophenol, dichlorophenoxyacetic acid, and lambda-cyhalothrin. Imprinted polymer-based MHNTs showed an excellent binding capacity of 246.73 mg g<sup>-1</sup> toward

trichlorophenol. Hydrogen bonds between trichlorophenol and methacrylic acid were the dominant recognition mechanism (Pan et al., 2011). In order to monitor the recognition and release of the analyte by imprinted materials, N-isopropylacrylamide (NIPAM) as a temperature-responsive monomer was used to prepare temperature-responsive, molecularly imprinted MHNTs. The maximum adsorption capacity of trichlorophenol was 197.7 mg g<sup>-1</sup> at 60°C and its release was at 20°C (Pan et al., 2012a, b). In work by Zhong et al. (2014), 4-vinylpyridine was used as a monomer and divinylbenzene as a cross-linker to prepare MHNTs-MIPs for removal of dichlorophenoxyacetic acid from a real sample. The recovery of analyte in <30 min by the MHNTs-MIPs-HPLC method was ~85–94% (Zhong et al., 2014) which was greater than that of CNTs-MIP where the recovery was <81%

due to the retaining capacity of analyte in the lumen of HNTs, which does not exist in CNTs (Yang et al., 2013b).

Lambda-cyhalothrin is a non-systemic pyrethroid insecticide and is highly active against a broad spectrum of pests in agriculture. Lambda-cyhalothrin residues in the environment have an adverse effect on human life because they can harm the central nervous system (Garcia et al., 2011). Thus, the detection and removal of these pollutants are very important (Pan et al., 2014). MHNTs-MIPs prepared by Pickering emulsion polymerization using MAA as a monomer showed better specific recognition and selectivity for lambda-cyhalothrin in a mixed solution with a relatively large adsorption capacity of 25 mg g<sup>-1</sup> (Hang et al., 2013). The use of MHNTs-MIPs for solid-phase extraction of pyrethroid in real samples warrants further research.

### Separation of Proteins

The extraction of purified proteins has attracted considerable interest because of their increasing significance in various applications ranging from diagnostics to therapeutics (Pei et al., 2009). The performance of the MHNTs-MIP for protein removal was investigated in various reports. For example, imprinted polydopamine on the surface of hydrophobic MHNTs prepared by Pickering emulsion polymerization showed a greater adsorption capacity (350 mg g<sup>-1</sup> at 0.7 mg L<sup>-1</sup>) of bovine hemoglobin and better affinity than non-imprinted polymers with a high imprinting factor of 3.24. Hydrophobic interaction, electrostatic interaction,  $\pi$ - $\pi$  bonds, and van der Waals forces are the main interactions between the cavity formed and the target protein (Sun et al., 2016). The adsorption capacity of MHNTs-MIPs is greater than other MIPs prepared by dopamine (Jia et al., 2013; Shen et al., 2012) which may be attributed to the more available binding site in the lumen of HNTs and magnetic NPs. On the other hand, compared to imprinted polydopamine-MHNTs, bovine serum albumin was retained less by MHNTs-MIPs prepared by N-isopropylacrylamide and methacrylic acid as bifunctional monomers (Zhu et al., 2015) or by N-isopropylacrylamide (NIPAM), acrylic amide (AAM), and N-(3-aminopropyl) methyl acrylamide hydrochloride (APM) as functional co-monomers

(Li et al., 2020a), proving that dopamine is a suitable monomer for protein recognition.

### Separation of Mycotoxins

Mycotoxins are toxic metabolites produced by fungi on crops such as maize, sorghum, and wheat and they have adverse effects on humans and animals due to their toxicity and carcinogenic effects (Wang et al., 2020a). Mycotoxins may result in an economic crisis if they are not detected and removed from food samples (Zain, 2011).

Recently, MHNTs-MIPs were used successfully for the detection and extraction of some mycotoxins, e.g. sterigmatocystin and zearalenone from food samples. As proof of concept, the limit of detection of zearalenone in maize samples using pseudo-hollow MHNTs-MIPs-coupled HPLC with a fluorescence detector (HPLC-FLD) method was 2.5 ng mL<sup>-1</sup> with satisfactory recoveries ranging from 74.95 to 88.41%. The chromatogram of the real sample after zearalenone removal, using the aforementioned method, contained some impurities which did not exist in the chromatogram of the immunoaffinity column (IAC). However, the retention time of analyte is not affected (Huang et al., 2020). In addition, a one-time use column and high cost are considered as drawbacks which limit IAC applications (Wang et al., 2020a). Consequently, MHNTs-MIPs used as stable, low-cost, and simple methods proved to be promising techniques for mycotoxins removal from food samples.

Thermo-responsive MHNTs-MIP and MCNTs-MIP showed greater affinity for sterigmatocystin than MCNTs-MIPs which may be attributed to the possibility of destroying the structures as well as the mechanical properties of the MCNTs after carboxylation modification, which affects the adsorption property of MCNTs-MIPs. Consequently, HNTs are a good alternative to CNTs. Furthermore, HNTs are cheap and readily available without complex fabrication, unlike CNTs (Wang et al., 2020b).

### MHNT and MHNT Nanocomposites for Extraction and Detection of Phenol and Polycyclic Aromatic Hydrocarbons

Organic pollutants, such as polycyclic aromatic hydrocarbons (PAHs) and phenolic compounds, are listed as priority contaminants in wastewater, food,

and soil with toxic effects on both plants and animals. The remediation of these toxic compounds has been an active area of research in the field of environmental science (Zango et al., 2020). Various studies have investigated the application of MHNT nanocomposites as potential adsorbents for these pollutants.  $\gamma$ -Fe<sub>2</sub>O<sub>3</sub>/HNTs removed phenol efficiently from aqueous solutions with a relatively acceptable adsorption capacity of 24.33 mg g<sup>-1</sup> and high regeneration ability where the composite could remove ~80% of phenol even after five adsorption/desorption cycles (Mirbagheri & Sabbaghi, 2018). A hybrid nanocomposite with MHNTs, polyaniline, and copper (MHNT-PANI-Cu) exhibited a better removal capacity of nitrated polycyclic aromatic hydrocarbons (nitrophenanthrenes) than MHNTs; this was attributed to the following: (1) PANI can interact with analytes via  $\pi$ - $\pi$  and hydrophobic interactions; and (2) transference between  $\pi$  electrons of nitrophenanthrenes and copper. The detection limit of MHNT-PANI-Cu-coupled Gas Chromatography-Mass Spectrometry (GC-MS) was 0.25 ng L<sup>-1</sup> in soil and wastewater samples after <1 min of extraction (Darvishnejad & Ebrahimzadeh, 2018) which is more sensitive than the MHNT-PANI-GC/MS method whereby the LODs of polycyclic aromatic hydrocarbons in beer sample were in the range 1.64–14.20 ng L<sup>-1</sup> (Shi et al., 2020). In conclusion, modifying MHNTs with PANI-Cu composites plays a vital role in the enhancement of extraction efficiency of organic pollutants.

## Conclusions and Future Perspectives

This review presents a snapshot of the current state of research on MHNTs and the efforts that govern their development in analytical fields. Firstly, the design strategies of MHNTs were clarified, including in situ growth, nano-encapsulation, and direct mixing methods. Meanwhile, the synthesis conditions, saturation magnetization, and the size of MNP of the MHNTs prepared by various methods have been summarized in the tables, which allows the reader to choose the appropriate synthesis approach based on the experimental demand. In addition, the common identification methods and characteristics of MHNTs have been described briefly, and these can be used to verify the successful synthesis of MHNTs. The surface functionalization of MHNTs is an important step in

improving their properties (such as adsorption efficiency, stability, and selectivity) and even endows them with new properties (such as electrochemical properties). Therefore, the surface functional modification from the types of functional agents and their combination modes with MHNTs have been introduced in detail. Finally, the analytical applications of MHNT and MHNT nanocomposites were reviewed. The main analytes extracted (mentioned here) include antibiotics, pesticides, proteins, carcinogens such as polycyclic aromatic hydrocarbons (PAHs), dyes, radioactive ions, and heavy metal ions such as Cu(II), Cd(II), Pb(II), Hg(II), Cr(III), and Cr(VI), found in environmental, biological, and food matrices.

Although research on MHNTs has made great advances, the following problems and challenges in its preparation still need to be resolved.

- (1) Shape heterogeneity of MNPs on the surface of HNTs. Fortunately, the present review has shown that by comparing the characteristics of various synthesis approaches, the most appropriate method can be selected to reduce shape heterogeneity. To avoid agglomeration and further reduce heterogeneity, the strong recommendation that emerged is to use a mass ratio of iron salts to HNTs in the range of 1:1 to 3:1 and an agitation time of 4 h in the synthesis.
- (2) Excess use of harmful products in the preparation of MHNTs. The review revealed that synthesis strategies can be simplified further and optimized based on the theories of conventional techniques.
- (3) The effect of agitation speed on the physicochemical characteristics of MHNTs should be explored further. When the problems above in the preparation of MHNTs are solved, and then they are functionalized to form complexes, better properties and wider applications can be achieved. For example, MHNT composites showed a maximum adsorption capacity and satisfactory extraction performance for the aforementioned analytes. In particular, MHNTs offered promise as an adsorbent for the removal of uranium. Hence, the elimination of other toxic radioactive ions, such as europium and iodine, by MHNTs composites could warrant further research. Compared with conventional SPE adsorbents, the integration of MNPs with HNTs can offer extra advantages such as very stable structural forms and rapid extrac-

tion from the sample medium. The modification of MHNTs by imprinted polymers means that this nanomaterial has a high selectivity and plays a vital role in the enhancement of the extraction efficiency of organic pollutants. On the other hand, MHNTs-MIPs bound by magnetic graphene oxide are promising as a potential magnetic solid-phase extraction agent. Thus, further research on the preparation of MGO/MHNTs-MIPs using green monomers and their application for the enrichment and extraction of various kinds of analytes in real samples needs to be explored.

**Acknowledgements** The authors acknowledge the financial support of the University Research-Training Projects of Algeria through the Grant No. A16N01UN440120220001.

**Funding** Funding sources are as stated in the Acknowledgements.

#### Declarations

**Competing Interest** The authors declare that they have no known competing financial interests or personal relationships that could have appeared to influence the work reported in this paper.

#### References

- Abhinayaa, R., Jeevitha, G., Mangalaraj, D., Ponpandian, N., Vidhya, K., & Angayarkanni, J. (2018). Cytotoxic consequences of Halloysite nanotube/iron oxide nanocomposite and iron oxide nanoparticles upon interaction with bacterial, non-cancerous and cancerous cells. *Colloids and Surfaces b: Biointerfaces*, *169*, 395–403.
- Abhinayaa, R., Jeevitha, G., Mangalaraj, D., Ponpandian, N., & Meena, P. (2019). Toxic influence of pristine and surfactant modified halloysite nanotubes on phytopathogenic bacteria. *Applied Clay Science*, *174*, 57–68.
- Afkhami, A., Sayari, S., Soltani-Felehgari, F., & Madrakian, T. (2015). Ni<sub>0.5</sub>Zn<sub>0.5</sub>Fe<sub>2</sub>O<sub>4</sub> nanocomposite-modified carbon paste electrode for highly sensitive and selective simultaneous electrochemical determination of trace amounts of mercury (II) and cadmium (II). *Journal of the Iranian Chemical Society*, *12*(2), 257–265.
- Afzali, D., & Fayazi, M. (2016). Deposition of MnO<sub>2</sub> nanoparticles on the magnetic halloysite nanotubes by hydrothermal method for lead (II) removal from aqueous solutions. *Journal of the Taiwan Institute of Chemical Engineers*, *63*, 421–429.
- Ahangaran, F., & Navarchian, A. H. (2020). Recent advances in chemical surface modification of metal oxide nanoparticles with silane coupling agents: A review. *Advances in Colloid and Interface Science*, 102298.
- Alguacil, F. J., Alcaraz, L., García-Díaz, I., & López, F. A. (2018). Removal of Pb<sup>2+</sup> in wastewater via adsorption onto an activated carbon produced from winemaking waste. *Metals*, *8*(9), 697.
- Amjadi, M., Samadi, A., & Manzoori, J. L. (2015a). A composite prepared from halloysite nanotubes and magnetite (Fe<sub>3</sub>O<sub>4</sub>) as a new magnetic sorbent for the preconcentration of cadmium (II) prior to its determination by flame atomic absorption spectrometry. *Microchimica Acta*, *182*(9), 1627–1633.
- Amjadi, M., Samadi, A., Manzoori, J. L., & Arsalani, N. (2015b). 5-(p-Dimethylaminobenzylidene) rhodanine-modified magnetic halloysite nanotubes as a new solid phase sorbent for silver ions. *Analytical Methods*, *7*(14), 5847–5853.
- Ashrafzadeh Afshar, E., Taher, M. A., & Fazelirad, H. (2017). Ultra-trace determination of thallium(I) using a nanocomposite consisting of magnetite, halloysite nanotubes and dibenzo-18-crown-6 for preconcentration prior to its quantitation by ET-AAS. *Microchimica Acta*. <https://doi.org/10.1007/s00604-016-2040-z>
- Aylaz, G., Kuhn, J., Lau, E. C., Yeung, C. C., Roy, V. A., Duman, M., & Yiu, H. H. (2021). Recent developments on magnetic molecular imprinted polymers (MMIPs) for sensing, capturing, and monitoring pharmaceutical and agricultural pollutants. *Journal of Chemical Technology & Biotechnology*. <https://doi.org/10.1002/jctb.6681>
- Bai, Y., Park, I. S., Lee, S. J., Bae, T. S., Watari, F., Uo, M., & Lee, M. H. (2011). Aqueous dispersion of surfactant-modified multiwalled carbon nanotubes and their application as an antibacterial agent. *Carbon*, *49*(11), 3663–3671.
- Bilici, M., Badak, M. U., Zengin, A., Suludere, Z., & Aktas, N. (2020). Synthesis of magnetic halloysite nanotube-based molecularly imprinted polymers for sensitive spectrophotometric detection of metoclopramide in urine samples. *Materials Science and Engineering: C*, *106*, 110223.
- Chen, L., Zhou, C. H., Fiore, S., Tong, D. S., Zhang, H., Li, C. S., Ji, S. F., & Yu, W. H. (2016). Functional magnetic nanoparticle/clay mineral nanocomposites: preparation, magnetism and versatile applications. *Applied Clay Science*, *127*, 143163.
- Cheng, D., Dai, X., Chen, L., Cui, Y., Qiang, C., Sun, Q., & Dai, J. (2019). Thiol-yne click synthesis of polyamide-amine dendritic magnetic halloysite nanotubes for the efficient removal of Pb (II). *ACS Sustainable Chemistry & Engineering*, *8*(2), 771–781.
- Dai, J., Wei, X., Cao, Z., Zhou, Z., Yu, P., Pan, J., Zou, T., Li, C., & Yan, Y. (2014). Highly-controllable imprinted polymer nanoshell at the surface of magnetic halloysite nanotubes for selective recognition and rapid adsorption of tetracycline. *RSC advances*, *4*(16), 7967. <https://doi.org/10.1039/c3ra45779f>
- Darvishnejad, M., & Ebrahimzadeh, H. (2018). Magnetic halloysite nanotube/polyaniline/copper composite coupled with gas chromatography-mass spectrometry: A rapid approach for determination of nitro-phenanthrenes in water and soil samples. *Journal of Chromatography A*, *1563*, 1–9.
- Das, K., Maiti, S., Ghosh, M., Mandal, D., & Das, P. K. (2013). Graphene oxide in cetyltrimethylammonium

- bromide (CTAB) reverse micelle: A befitting soft nanocomposite for improving efficiency of surface-active enzymes. *Journal of Colloid and Interface Science*, 395, 111–118.
- Di, S., Ning, T., Yu, J., Chen, P., Yu, H., Wang, J., Yang, H., & Zhu, S. (2020). Recent advances and applications of magnetic nanomaterials in environmental sample analysis. *TrAC Trends in Analytical Chemistry*, 126, 115864.
- Dramou, P., Fizir, M., Taleb, A., Itatahine, A., Dahiru, N. S., Mehdi, Y. A., Wei, L., Zhang, J., & He, H. (2018). Folic acid-conjugated chitosan oligosaccharide-magnetic halloysite nanotubes as a delivery system for camptothecin. *Carbohydrate Polymers*, 197, 117–127.
- Dramou, P., Wang, F., Sun, Y., Zhang, J., Yang, P., Liu, D., & He, H. (2022). Synthesis and characterization of superparamagnetic graphene oxide assembled halloysite composites for extraction of rutin. *Applied Clay Science*, 217, 106397.
- Dramou, P., Zuo, P., He, H., Pham-Huy, L. A., Zou, W., Xiao, D., & Pham-Huy, C. (2013). Development of novel amphiphilic magnetic molecularly imprinted polymers compatible with biological fluids for solid phase extraction and physicochemical behavior study. *Journal of Chromatography A*, 1317, 110–120.
- Duan, J., Liu, R., Chen, T., Zhang, B., & Liu, J. (2012). Halloysite nanotube-Fe<sub>3</sub>O<sub>4</sub> composite for removal of methyl violet from aqueous solutions. *Desalination*, 293, 46–52. <https://doi.org/10.1016/j.desal.2012.02.022>
- Duan, X.-L., Yuan, C.-G., Guo, Q., Niu, S.-L., He, K.-Q., & Xia, G.-W. (2021). Preparation of halloysite nanotubes-encapsulated magnetic microspheres for elemental mercury removal from coal-fired flue gas. *Journal of Hazardous Materials*, 406, 124683.
- Eskandarloo, H., Arshadi, M., & Abbaspourrad, A. (2018). Magnetic dendritic halloysite nanotube for highly selective recovery of heparin digested from porcine intestinal mucosa. *ACS Sustainable Chemistry & Engineering*, 6(11), 14561–14573.
- Fakhrullin, R. F., & Lvov, Y. M. (2016). Halloysite clay nanotubes for tissue engineering. *Nanomedicine*, 11(17), 2243–2246. <https://doi.org/10.2217/nnm-2016-0250>
- Farooq, M. U., & Jalees, M. I. (2020). Application of magnetic graphene oxide for water purification: Heavy metals removal and disinfection. *Journal of Water Process Engineering*, 33, 101044.
- Fayazi, M., Taher, M. A., Afzali, D., & Mostafavi, A. (2016). Fe<sub>3</sub>O<sub>4</sub> and MnO<sub>2</sub> assembled on halloysite nanotubes: A highly efficient solid-phase extractant for electrochemical detection of mercury (II) ions. *Sensors and Actuators b: Chemical*, 228, 1–9.
- Fizir, M., Dramou, P., Zhang, K., Sun, C., Pham-Huy, C., & He, H. (2017). Polymer grafted-magnetic halloysite nanotube for controlled and sustained release of cationic drug. *Journal of Colloid and Interface Science*, 505, 476–488.
- Fizir, M., Dramou, P., Nasiru Sintali, D., Ruya, W., Huang, T., & He, H. (2018a). Halloysite nanotubes in analytical sciences and in drug delivery: A review. *Microchimica Acta*, 185, article number 389, <https://doi.org/10.1007/s00604-018-2908-1>.
- Fizir, M., Wei, L., Muchuan, N., Itatahine, A., mehdi, Y. A., He, H., & Dramou, P. (2018b). QbD approach by computer aided design and response surface methodology for molecularly imprinted polymer based on magnetic halloysite nanotubes for extraction of norfloxacin from real samples. *Talanta*, 184, 266–276. <https://doi.org/10.1016/j.talanta.2018b.02.056>
- Fizir, M., Richa, A., He, H., Touil, S., Brada, M., & Fizir, L. (2020). A mini review on molecularly imprinted polymer based halloysite nanotubes composites: Innovative materials for analytical and environmental applications. *Reviews in Environmental Science and Biotechnology*, 19, 241–258.
- Fizir, M., Dahiru, N. S., Cui, Y., Zhi, H., Dramou, P., & He, H. (2021). Simple and Efficient Detection Approach of Quercetin from Biological Matrix by Novel Surface Imprinted Polymer Based Magnetic Halloysite Nanotubes Prepared by a Sol-Gel Method. *Journal of Chromatographic Science*, 59, 681–695. <https://doi.org/10.1093/chromsci/bmaa120>
- Foroughirad, S., Haddadi-Asl, V., Khosravi, A., & Salami-Kalajahi, M. (2020a). Effect of porogenic solvent in synthesis of mesoporous and microporous molecularly imprinted polymer based on magnetic halloysite nanotubes. *Materials Today Communications*, 101780.
- Foroughirad, S., Haddadi-Asl, V., Khosravi, A., & Salami-Kalajahi, M. (2020b). Synthesis of magnetic nanoparticles-decorated halloysite nanotubes/poly ([2-(acryloyloxy) ethyl] trimethylammonium chloride) hybrid nanoparticles for removal of Sunset Yellow from water. *Journal of Polymer Research*, 27(10), 1–10.
- Foroughirad, S., Haddadi-Asl, V., Khosravi, A., & Salami-Kalajahi, M. (2021). Magnetic halloysite-based molecularly imprinted polymer for specific recognition of sunset yellow in dyes mixture. *Polymers for Advanced Technologies*, 32(2), 803–814.
- Fu, H., Liao, L., Li, X., & Chen, W. (2016). Preparation and characterization of novel modified halloysite-Fe<sub>3</sub>O<sub>4</sub>-Ag/polyurea nanocomposites with antibacterial property. *International Journal of Polymeric Materials and Polymeric Biomaterials*, 65(17), 863–871.
- Gabal, M., El-Shishtawy, R. M., & Al Angari, Y. (2012). Structural and magnetic properties of nano-crystalline Ni-Zn ferrites synthesized using egg-white precursor. *Journal of Magnetism and Magnetic Materials*, 324(14), 2258–2264.
- Gabal, M. A. (2010). Magnetic properties of NiCuZn ferrite nanoparticles synthesized using egg-white. *Materials Research Bulletin*, 45(5), 589–593.
- Gan, M., Huang, Y., Zhang, Y., Pan, J., Shi, W., & Yan, Y. (2015). Fabrication of Ag/halloysite nanotubes/Fe<sub>3</sub>O<sub>4</sub> nanocatalyst and their catalytic performance in 4-nitrophenol reduction. *Desalination and Water Treatment*, 56(2), 425–434.
- Ganganboina, A. B., Chowdhury, A. D., & Doong, R.-A. (2017). Nano assembly of N-doped graphene quantum dots anchored Fe<sub>3</sub>O<sub>4</sub>/halloysite nanotubes for high performance supercapacitor. *Electrochimica Acta*, 245, 912–923.
- Gao, C., Li, W., Morimoto, H., Nagaoka, Y., & Maekawa, T. (2006). Magnetic carbon nanotubes: Synthesis by electrostatic self-assembly approach and application in bio-manipulations. *The Journal of Physical Chemistry B*, 110(14), 7213–7220.

- Gao, C., Lyu, F., & Yin, Y. (2020). Encapsulated metal nanoparticles for catalysis. *Chemical Reviews*.
- Gao, F. (2019). An overview of surface-functionalized magnetic nanoparticles: Preparation and application for wastewater treatment. *ChemistrySelect*, 4(22), 6805–6811.
- Garcia, M., Scheffczyk, A., Garcia, T., & Römbke, J. (2011). The effects of the insecticide lambda-Cyhalothrin on the earthworm *Eisenia fetida* under experimental conditions of tropical and temperate regions. *Environmental Pollution*, 159(2), 398–400.
- Ghandi, K. (2014). A review of ionic liquids, their limits and applications. *Green and Sustainable Chemistry*, 4, 44–53.
- Guan, W., Wang, X., Pan, J., Lei, J., Zhou, Y., Lu, C., & Yan, Y. (2012). Synthesis of magnetic halloysite composites for the effective removal of tetracycline hydrochloride from aqueous solutions. *Adsorption Science & Technology*, 30(7), 579–591.
- Guć, M., Messyas, B., & Schroeder, G. (2021). Environmental impact of molecularly imprinted polymers used as anolyte sorbents in mass spectrometry. *Science of the Total Environment*, 772, 145074.
- Hajizadeh, Z., & Maleki, A. (2018). Poly (ethylene imine)-modified magnetic halloysite nanotubes: A novel, efficient and recyclable catalyst for the synthesis of dihydropyrano [2, 3-c] pyrazole derivatives. *Molecular Catalysis*, 460, 87–93.
- Hajizadeh, Z., Hassanzadeh-Afruzi, F., Jelodar, D. F., Ahghari, M. R., & Maleki, A. (2020a). Cu (ii) immobilized on Fe<sub>3</sub>O<sub>4</sub>@HNTs-tetrazole (CFHT) nanocomposite: Synthesis, characterization, investigation of its catalytic role for the 1, 3 dipolar cycloaddition reaction, and antibacterial activity. *RSC Advances*, 10(44), 26467–26478.
- Hajizadeh, Z., Maleki, A., Rahimi, J., & Eivazzadeh-Keihan, R. (2020b). Halloysite nanotubes modified by Fe<sub>3</sub>O<sub>4</sub> nanoparticles and applied as a natural and efficient nanocatalyst for the symmetrical hantzsch reaction. *Silicon*, 12(5), 1247–1256.
- Hamza, H., Ferretti, A. M., Innocenti, C., Fidecka, K., Licandro, E., Sangregorio, C., & Maggioni, D. (2020). An Approach for Magnetic Halloysite Nanocomposite with Selective Loading of Superparamagnetic Magnetite Nanoparticles in the Lumen. *Inorganic Chemistry*, 59(17), 12086–12096.
- Hang, H., Li, C., Pan, J., Li, L., Dai, J., Dai, X., Yu, P., & Feng, Y. (2013). Selective separation of lambda-cyhalothrin by porous/magnetic molecularly imprinted polymers prepared by Pickering emulsion polymerization. *Journal of Separation Science*, 36(19), 3285–3294.
- He, J., Zou, T., Chen, X., Dai, J., Xie, A., Zhou, Z., & Yan, Y. (2016a). Magnetic organic-inorganic nanocomposite with ultrathin imprinted polymers via an in situ surface-initiated approach for specific separation of chloramphenicol. *RSC Advances*, 6(74), 70383–70393.
- He, W., Chen, Y., Zhang, W., Hu, C., Wang, J., & Wang, P. (2015). Removal of UO<sub>2</sub><sup>2+</sup> from aqueous solution using halloysite nanotube-Fe<sub>3</sub>O<sub>4</sub> composite. *Korean Journal of Chemical Engineering*, 33(1), 170–177. <https://doi.org/10.1007/s11814-015-0111-1>
- He, W., Chen, Y., Zhang, W., Hu, C., Wang, J., & Wang, P. (2016b). Removal of UO<sub>2</sub><sup>2+</sup> from aqueous solution using halloysite nanotube-Fe<sub>3</sub>O<sub>4</sub> composite. *Korean Journal of Chemical Engineering*, 33(1), 170–177.
- He, Y., Yi, C., Zhang, X., Zhao, W., & Yu, D. (2021). Magnetic graphene oxide: Synthesis approaches, physico-chemical characteristics, and biomedical applications. *TrAC Trends in Analytical Chemistry*, 116191.
- Huang, Z., He, J., Li, H., Zhang, M., Wang, H., Zhang, Y., Li, Y., You, L., & Zhang, S. (2020). Synthesis and application of magnetic-surfaced pseudo molecularly imprinted polymers for zearalenone pretreatment in cereal samples. *Food Chemistry*, 308, 125696.
- Itatahine, A., Mehdi, Y. A., Fizir, M., Qi, M., Dramou, P., & He, H. (2017). Multifunctional carbon nanomaterials for camptothecin low-water soluble anticancer drug delivery. *New Journal of Chemistry*.
- Jee, S.-C., Kim, M., Shinde, S. K., Ghodake, G. S., Sung, J.-S., & Kadam, A. A. (2020). Assembling ZnO and Fe<sub>3</sub>O<sub>4</sub> nanostructures on halloysite nanotubes for antibacterial assessments. *Applied Surface Science*, 509, 145358.
- Jia, L., Zhou, T., Xu, J., Li, F., Xu, Z., Zhang, B., Guo, S., Shen, X., & Zhang, W. (2017). AuPd bimetallic nanocrystals embedded in magnetic halloysite nanotubes: Facile synthesis and catalytic reduction of nitroaromatic compounds. *Nanomaterials*, 7(10), 333.
- Jia, L., Zhou, T., Xu, J., Li, X., Dong, K., Huang, J., & Xu, Z. (2016). The enhanced catalytic activities of asymmetric Au-Ni nanoparticle decorated halloysite-based nanocomposite for the degradation of organic dyes. *Nanoscale Research Letters*, 11(1), 1–7.
- Jia, P., Ma, Y., Rahman, R., & Ma, Y. (2011). Synthesis of Magnetic Ferriferrous Oxide/Halloysite Composite. *Integrated Ferroelectrics*, 127(1), 116–120.
- Jia, X., Xu, M., Wang, Y., Ran, D., Yang, S., & Zhang, M. (2013). Polydopamine-based molecular imprinting on silica-modified magnetic nanoparticles for recognition and separation of bovine hemoglobin. *The Analyst*, 138(2), 651–658.
- Jiang, L., Zhang, C., Wei, J., Tjiu, W., Pan, J., Chen, Y., & Liu, T. (2014a). Surface modifications of halloysite nanotubes with superparamagnetic Fe<sub>3</sub>O<sub>4</sub> nanoparticles and carbonaceous layers for efficient adsorption of dyes in water treatment. *Chemical Research in Chinese Universities*, 30(6), 971–977. <https://doi.org/10.1007/s40242-014-4218-4>
- Jiang, L., Zhang, C., Wei, J., Tjiu, W., Pan, J., Chen, Y., & Liu, T. (2014b). Surface modifications of halloysite nanotubes with superparamagnetic Fe<sub>3</sub>O<sub>4</sub> nanoparticles and carbonaceous layers for efficient adsorption of dyes in water treatment. *Chemical Research in Chinese Universities*, 30(6), 971–977.
- Jomova, K., Jenisova, Z., Feszterova, M., Baros, S., Liska, J., Hudecova, D., Rhodes, C. J., & Valko, M. (2011). Arsenic: Toxicity, oxidative stress and human disease. *Journal of Applied Toxicology*, 31(2), 95–107.
- Joussein, E., Petit, S., Churchman, J., Theng, B., Righi, D., & Delvaux, B. (2005). Halloysite clay minerals—A review. *Clay Minerals*, 40, 383–426.

- Kadam, A. A., Jang, J., & Lee, D. S. (2017). Supermagnetically tuned halloysite nanotubes functionalized with aminosilane for covalent laccase immobilization. *ACS Applied Materials & Interfaces*, 9(18), 15492–15501.
- Kadam, A. A., Jang, J., Jee, S. C., Sung, J.-S., & Lee, D. S. (2018). Chitosan-functionalized supermagnetic halloysite nanotubes for covalent laccase immobilization. *Carbohydrate Polymers*, 194, 208–216.
- Kadam, A. A., Sharma, B., Shinde, S. K., Ghodake, G. S., Saratale, G. D., Saratale, R. G., Kim, D. Y., & Sung, J. S. (2020a). Thiolation of Chitosan Loaded over Supermagnetic Halloysite Nanotubes for Enhanced Laccase Immobilization. *Nanomaterials*, 10(12), 2560.
- Kadam, A. A., Shinde, S. K., Ghodake, G. S., Saratale, G. D., Saratale, R. G., Sharma, B., Hyun, S., & Sung, J. S. (2020b). Chitosan-Grafted Halloysite Nanotubes-Fe<sub>3</sub>O<sub>4</sub> Composite for Laccase-Immobilization and Sulfamethoxazole-Degradation. *Polymers*, 12(10), 2221.
- Kharisova, O. V., Dias, H. R., & Kharisov, B. I. (2015). Magnetic adsorbents based on micro- and nano-structured materials. *RSC Advances*, 5(9), 6695–6719.
- Khunová, V., Šafařík, I., Škrátek, M., Kelnar, I., & Tomanová, K. (2016). Biodegradable polymer nanocomposites based on natural nanotubes: Effect of magnetically modified halloysite on the behaviour of polycaprolactone. *Clay Minerals*, 51(3), 435–444.
- Khunová, V., Pavliňáková, V., Škrátek, M., Šafařík, I., & Pavliňák, D. (2018). Magnetic halloysite reinforced biodegradable nanofibres: new challenge for medical applications. AIP Conference Proceedings.
- Kim, M., Jee, S. C., Sung, J.-S., & Kadam, A. A. (2018). Antiproliferative applications of laccase immobilized on supermagnetic chitosan-functionalized halloysite nanotubes. *International Journal of Biological Macromolecules*, 118, 228–237.
- Konnova, S., Lvov, Y., & Fakhruddin, R. (2016). Magnetic halloysite nanotubes for yeast cell surface engineering. *Clay Minerals*, 51(3), 429–438.
- Kurmoo, M. (2009). Magnetic metal-organic frameworks. *Chemical Society Reviews*, 38(5), 1353–1379.
- Lee, Y.-J., Lee, S.-C., Jee, S. C., Sung, J.-S., & Kadam, A. A. (2019). Surface functionalization of halloysite nanotubes with supermagnetic iron oxide, chitosan and 2-D calcium-phosphate nanoflakes for synergistic osteoconduction enhancement of human adipose tissue-derived mesenchymal stem cells. *Colloids and Surfaces b: Biointerfaces*, 173, 18–26.
- Li, F., Huang, Y., Huang, K., Lin, J., & Huang, P. (2020a). Functional magnetic graphene composites for biosensing. *International Journal of Molecular Sciences*, 21(2), 390.
- Li, G., Zha, J., Niu, M., Hu, F., Hui, X., Tang, T., Fizir, M., & He, H. (2018a). Bifunctional monomer molecularly imprinted sol-gel polymers based on the surface of magnetic halloysite nanotubes as an effective extraction approach for norfloxacin. *Applied Clay Science*, 162, 409–417.
- Li, L., Wang, F., Lv, Y., Liu, J., Zhang, D., & Shao, Z. (2018b). Halloysite nanotubes and Fe<sub>3</sub>O<sub>4</sub> nanoparticles enhanced adsorption removal of heavy metal using electrospun membranes. *Applied Clay Science*, 161, 225–234.
- Li, X., Chen, J., Liu, H., Deng, Z., Li, J., Ren, T., Huang, L., Chen, W., Yang, Y., & Zhong, S. (2019).  $\beta$ -Cyclodextrin coated and folic acid conjugated magnetic halloysite nanotubes for targeting and isolating of cancer cells. *Colloids and Surfaces B: Biointerfaces*, 181, 379–388.
- Li, X., Liu, H., Deng, Z., Chen, W., Li, T., Zhang, Y., He, Y., Tan, Z., & Zhong, S. (2020b). PEGylated Thermo-Sensitive Bionic Magnetic Core-Shell Structure Molecularly Imprinted Polymers Based on Halloysite Nanotubes for Specific Adsorption and Separation of Bovine Serum Albumin. *Polymers*, 12(3), 536.
- Li, Y., Yuan, X., Jiang, L., Dai, H., Zhao, Y., Guan, X., Bai, J., & Wang, H. (2022). Manipulation of halloysite clay nanotube lumen for environmental remediation: A review. *Environmental Science: Nano*.
- Liang, M., Chen, R., Xian, Y., Hu, J., Hou, X., Wang, B., Wu, Y., & Wang, L. (2021). Determination of bongkreikic acid and isobongkreikic acid in rice noodles by HPLC-Orbitrap HRMS technology using magnetic halloysite nanotubes. *Food chemistry*, 344, 128682.
- Liu, M., Jia, Z., Jia, D., & Zhou, C. (2014). Recent advance in research on halloysite nanotubes-polymer nanocomposite. *Progress in Polymer Science*, 39(8), 1498–1525.
- Liu, W., Fizir, M., Hu, F., Li, A., Hui, X., Zha, J., & He, H. (2018a). Mixed hemimicelle solid-phase extraction based on magnetic halloysite nanotubes and ionic liquids for the determination and extraction of azo dyes in environmental water samples. *Journal of Chromatography A*, 1551, 10–20.
- Liu, W., Wang, R., Hu, F., Wu, P., Huang, T., Fizir, M., & He, H. (2018b). Novel mixed hemimicelles based on non-ionic surfactant-imidazolium ionic liquid and magnetic halloysite nanotubes as efficient approach for analytical determination. *Analytical and Bioanalytical Chemistry*, 410(28), 7357–7371.
- López-López, M., Durán, J., Delgado, A., & González-Caballero, F. (2005). Stability and magnetic characterization of oleate-covered magnetite ferrofluids in different non-polar carriers. *Journal of Colloid and Interface Science*, 291(1), 144–151.
- Lvov, Y. M., DeVilliers, M. M., & Fakhruddin, R. F. (2016). The application of halloysite tubule nanoclay in drug delivery. *Expert Opinion on Drug Delivery*, 13(7), 977–986. <https://doi.org/10.1517/17425247.2016.1169271>
- Lvov, Y. M., Shchukin, D. G., Mohwald, H., & Price, R. R. (2008). Halloysite clay nanotubes for controlled release of protective agents. *ACS Nano*, 2(5), 814–820. <https://doi.org/10.1021/mn800259q>
- Ma, P., Zhou, Z., Dai, J., Qin, L., Ye, X., Chen, X., Xie, A., Yan, Y., & Li, C. (2016a). A biomimetic *Setaria viridis*-inspired imprinted nanoadsorbent: green synthesis and application to the highly selective and fast removal of sulfamethazine. *RSC Advances*, 6(12), 9619–9630. <https://doi.org/10.1039/c5ra18715j>
- Ma, W., Dai, J., Dai, X., Da, Z., & Yan, Y. (2016b). Preparation and characterization of chitosan/halloysite magnetic microspheres and their application for removal of tetracycline from an aqueous solution. *Desalination and Water Treatment*, 57(9), 4162–4173. <https://doi.org/10.1080/19443994.2014.988653>



- Maensiri, S., Masingboon, C., Boonchom, B., & Seraphin, S. (2007). A simple route to synthesize nickel ferrite ( $\text{NiFe}_2\text{O}_4$ ) nanoparticles using egg white. *Scripta Materialia*, 56(9), 797–800.
- Majidi, S., Zeinali Sehgri, F., Farkhani, S. M., Soleymani Goloujeh, M., & Akbarzadeh, A. (2016). Current methods for synthesis of magnetic nanoparticles. *Artificial Cells, Nanomedicine, and Biotechnology*, 44(2), 722–734.
- Maleki, A., Hajizadeh, Z., & Firouzi-Haji, R. (2018). Eco-friendly functionalization of magnetic halloysite nanotube with  $\text{SO}_3\text{H}$  for synthesis of dihydropyrimidinones. *Microporous and Mesoporous Materials*, 259, 46–53.
- Maleki, A., Hajizadeh, Z., & Salehi, P. (2019). Mesoporous halloysite nanotubes modified by  $\text{CuFe}_2\text{O}_4$  spinel ferrite nanoparticles and study of its application as a novel and efficient heterogeneous catalyst in the synthesis of pyrazolopyridine derivatives. *Scientific Reports*, 9(1), 1–8.
- Mateo-Sagasta, J., Zadeh, S. M., Turrall, H., & Burke, J. (2017). Water pollution from agriculture: a global review. Executive summary. Food and Agriculture Organization of the United Nations: <https://www.fao.org/3/i7754e/i7754e.pdf>.
- Maziarz, P., & Matusik, J. (2017). Halloysite composites with  $\text{Fe}_3\text{O}_4$  particles: The effect of impregnation on the removal of aqueous Cd (II) and Pb (II). *Mineralogia*, 48, 107–126.
- Maziarz, P., Matusik, J., Leiviskä, T., Strączek, T., Kapusta, C., Woch, W. M., Tokarz, W., & Gorniak, K. (2019). Toward highly effective and easily separable halloysite-containing adsorbents: The effect of iron oxide particles impregnation and new insight into As (V) removal mechanisms. *Separation and Purification Technology*, 210, 390–401.
- Mirbagheri, N. S., & Sabbaghi, S. (2018). A natural kaolin/ $\gamma\text{-Fe}_2\text{O}_3$  composite as an efficient nano-adsorbent for removal of phenol from aqueous solutions. *Microporous and Mesoporous Materials*, 259, 134–141.
- Mu, B., Wang, W., Zhang, J., & Wang, A. (2014a). Superparamagnetic sandwich structured silver/halloysite nanotube/ $\text{Fe}_3\text{O}_4$  nanocomposites for 4-nitrophenol reduction. *RSC Advances*, 4(74), 39439–39445.
- Mu, B., Zhang, W., & Wang, A. (2014b). Facile fabrication of superparamagnetic coaxial gold/halloysite nanotubes/ $\text{Fe}_3\text{O}_4$  nanocomposites with excellent catalytic property for 4-nitrophenol reduction. *Journal of Materials Science*, 49(20), 7181–7191.
- Naumenko, E. A., Guryanov, I. D., Yendluri, R., Lvov, Y. M., & Fakhruллин, R. F. (2016). Clay nanotube-biopolymer composite scaffolds for tissue engineering. *Nanoscale*, 8(13), 7257–7271. <https://doi.org/10.1039/c6nr00641h>
- Nguyen, T. K. L., Cao, X. T., Park, C., & Lim, K. T. (2017). Preparation, characterization and application of magnetic halloysite nanotubes for dye removal. *Molecular Crystals and Liquid Crystals*, 644(1), 153–159.
- Nonkumwong, J., Ananta, S., & Srisombat, L. (2016). Effective removal of lead (II) from wastewater by amine-functionalized magnesium ferrite nanoparticles. *RSC Advances*, 6(53), 47382–47393.
- Pan, J., Yao, H., Xu, L., Ou, H., Huo, P., Li, X., & Yan, Y. (2011). Selective Recognition of 2,4,6-Trichlorophenol by Molecularly Imprinted Polymers Based on Magnetic Halloysite Nanotubes Composites. *The Journal of Physical Chemistry C*, 115(13), 5440–5449. <https://doi.org/10.1021/jp111120x>
- Pan, J., Hang, H., Dai, X., Dai, J., Huo, P., & Yan, Y. (2012a). Switched recognition and release ability of temperature responsive molecularly imprinted polymers based on magnetic halloysite nanotubes. *Journal of Materials Chemistry*, 22(33), 17167. <https://doi.org/10.1039/c2jm32821f>
- Pan, J., Wang, B., Dai, J., Dai, X., Hang, H., Ou, H., & Yan, Y. (2012b). Selective recognition of 2,4,5-trichlorophenol by temperature responsive and magnetic molecularly imprinted polymers based on halloysite nanotubes. *Journal of Materials Chemistry*, 22(8), 3360. <https://doi.org/10.1039/c1jm14825g>
- Pan, J., Zhu, W., Dai, X., Yan, X., Gan, M., Li, L., Hang, H., & Yan, Y. (2014). Magnetic molecularly imprinted microcapsules derived from Pickering emulsion polymerization and their novel adsorption characteristics for  $\lambda$ -cyhalothrin. *RSC Advances*, 4(9), 4435–4443.
- Pei, Y., Wang, J., Wu, K., Xuan, X., & Lu, X. (2009). Ionic liquid-based aqueous two-phase extraction of selected proteins. *Separation and Purification Technology*, 64(3), 288–295.
- Polat, G., & Açikel, Y. S. (2019). Synthesis and Characterization of Magnetic Halloysite-Alginate Beads for the Removal of Lead (II) Ions from Aqueous Solutions. *Journal of Polymers and the Environment*, 27(9), 1971–1987.
- Rajabi, H. R., Roushani, M., & Shamsipur, M. (2013). Development of a highly selective voltammetric sensor for nanomolar detection of mercury ions using glassy carbon electrode modified with a novel ion imprinted polymeric nanobeads and multi-wall carbon nanotubes. *Journal of Electroanalytical Chemistry*, 693, 16–22.
- Riahi-Madvaar, R., Taher, M. A., & Fazelirad, H. (2017). Synthesis and characterization of magnetic halloysite-iron oxide nanocomposite and its application for naphthol green B removal. *Applied Clay Science*, 137, 101–106. <https://doi.org/10.1016/j.clay.2016.12.019>
- Rios, A., Zougagh, M., & Bouri, M. (2013). Magnetic (nano) materials as a useful tool for sample preparation in analytical methods. A Review. *Analytical Methods*, 5(18), 4558–4573.
- Rouhi, M., Babamoradi, M., Hajizadeh, Z., Maleki, A., & Maleki, S. T. (2020). Design and performance of polypyrrole/halloysite nanotubes/ $\text{Fe}_3\text{O}_4$ /Ag/Co nanocomposite for photocatalytic degradation of methylene blue under visible light irradiation. *Optik*, 212, 164721.
- Sadjadi, S., Lazzara, G., Heravi, M. M., & Cavallaro, G. (2019). Pd supported on magnetic carbon coated halloysite as hydrogenation catalyst: Study of the contribution of carbon layer and magnetization to the catalytic activity. *Applied Clay Science*, 182, 105299.
- Selvaraj, M., Rajalakshmi, K., Ahn, D.-H., Yoon, S.-J., Nam, Y.-S., Lee, Y., Xu, Y., Song, J. W., & Lee, K. B. (2021). Tetraphenylethene-based fluorescent probe with aggregation-induced emission behavior for  $\text{Hg}^{2+}$  detection and its application. *Analytica Chimica Acta*, 1148, 238178.
- Shah, A., Nisar, A., Khan, K., Nisar, J., Niaz, A., Ashiq, M. N., & Akhter, M. S. (2019). Amino acid functionalized glassy carbon electrode for the simultaneous detection of thallium and mercuric ions. *Electrochimica Acta*, 321, 134658.

- Shen, X., Zhou, T., & Ye, L. (2012). Molecular imprinting of protein in Pickering emulsion. *Chemical Communications*, 48(66), 8198–8200.
- Shende, P., & Shah, P. (2021). Carbohydrate-based magnetic nanocomposites for effective cancer treatment. *International Journal of Biological Macromolecules*, 175, 281–293. <https://doi.org/10.1016/j.ijbiomac.2021.02.044>
- Shi, Z., Pang, W., Chen, M., Wu, Y., & Zhang, H. (2020). Polyaniline-Modified Magnetic Halloysite Nanotube-Based Magnetic Micro-Solid-Phase Extraction for the Analysis of Polycyclic Aromatic Hydrocarbons in Beer Samples by Gas Chromatography-Mass Spectrometry. *Food Analytical Methods*, 1–12.
- Siddeeg, S. M., Tahoon, M. A., Alsaiani, N. S., Shabbir, M., & Rehab, F. B. (2021). Application of Functionalized Nanomaterials as Effective Adsorbents for the Removal of Heavy Metals from Wastewater: A Review. *Current Analytical Chemistry*, 17(1), 4–22.
- Sillu, D., & Agnihotri, S. (2019). Cellulase immobilization onto magnetic halloysite nanotubes: Enhanced enzyme activity and stability with high cellulose saccharification. *ACS Sustainable Chemistry & Engineering*, 8(2), 900–913.
- Sohrabi, M. R., Matbouie, Z., Asgharinezhad, A. A., & Dehghani, A. (2013). Solid phase extraction of Cd (II) and Pb (II) using a magnetic metal-organic framework, and their determination by FAAS. *Microchimica Acta*, 180(7–8), 589–597.
- Song, X., Wang, Y., Zhou, L., Luo, X., & Liu, J. (2021). Halloysite nanotubes stabilized polyurethane foam carbon coupled with iron oxide for high-efficient and fast treatment of arsenic (III/V) wastewater. *Chemical Engineering Research and Design*, 165, 298–307.
- Song, X., Zhou, L., Zhang, Y., Chen, P., & Yang, Z. (2019). A novel cactus-like Fe<sub>3</sub>O<sub>4</sub>/Halloysite nanocomposite for arsenite and arsenate removal from water. *Journal of Cleaner Production*, 224, 573–582.
- Sun, Y., Chen, J., Li, Y., Li, H., Zhu, X., Hu, Y., Huang, S., Li, J., & Zhong, S. (2016). Bio-inspired magnetic molecularly imprinted polymers based on Pickering emulsions for selective protein recognition. *New Journal of Chemistry*, 40(10), 8745–8752.
- Taghizadeh, M., Asgharinezhad, A. A., Samkhaniy, N., Tadjarodi, A., Abbaszadeh, A., & Pooladi, M. (2014). Solid phase extraction of heavy metal ions based on a novel functionalized magnetic multi-walled carbon nanotube composite with the aid of experimental design methodology. *Microchimica Acta*, 181(5–6), 597–605.
- Tian, X., Wang, W., Tian, N., Zhou, C., Yang, C., & Komarneni, S. (2016). Cr(VI) reduction and immobilization by novel carbonaceous modified magnetic Fe<sub>3</sub>O<sub>4</sub>/halloysite nano-hybrid. *Journal of Hazardous Materials*, 309, 151–156. <https://doi.org/10.1016/j.jhazmat.2016.01.081>
- Todorov, P. T., & Ilieva, E. N. (2006). Contamination with uranium from natural and anthropological sources. *Romanian Journal of Physics*, 51(1/2), 27.
- Tsoufis, T., Katsaros, F., Kooi, B., Bletsas, E., Papageorgiou, S., Deligiannakis, Y., & Panagiotopoulos, I. (2017). Halloysite nanotube-magnetic iron oxide nanoparticle hybrids for the rapid catalytic decomposition of pentachlorophenol. *Chemical Engineering Journal*, 313, 466–474.
- Türkeş, E., & Açikel, Y. S. (2020). Synthesis and characterization of magnetic halloysite–chitosan nanocomposites: Use in the removal of methylene blue in wastewaters. *International Journal of Environmental Science and Technology*, 17(3), 1281–1294.
- Tušar, N., Kaucic, V., & Logar, N. (2013). Chapter 15 Functionalized Porous Silicates as Catalysts for Water and Air Purification. *New and Future Developments in Catalysis*; Suib, S.L., Ed.; Elsevier: Amsterdam, The Netherlands, 365–383.
- Vahidhabanu, S., Adeogun, A. I., & Babu, B. R. (2019). Biopolymer-grafted, magnetically tuned halloysite nanotubes as efficient and recyclable spongelike adsorbents for anionic azo dye removal. *ACS Omega*, 4(1), 2425–2436.
- Wan, X. Y., Zhan, Y. Q., Long, Z. H., Zeng, G. Y., & He, Y. (2017). Core@double-shell structured magnetic halloysite nanotube nano-hybrid as efficient recyclable adsorbent for methylene blue removal. *Chemical Engineering Journal*, 330, 491–504. <https://doi.org/10.1016/j.cej.2017.07.178>
- Wang, F., Ni, X., Zhang, J., Zhang, Q., Jia, H., He, H., & Dramou, P. (2022). Novel composite nanomaterials based on magnetic molecularly imprinted polymers for selective extraction and determination of rutin in fruit juice. *Food Chemistry*, 381, 132275.
- Wang, H., He, J., Song, L., Zhang, Y., Xu, M., Huang, Z., Jin, L., Ba, X., Li, Y., You, L., & Zhang, S. (2020a). Etching of Halloysite Nanotubes Hollow Imprinted Materials as Adsorbent for Extracting of Zearalenone from Grain Samples. *Microchemical Journal*, 104953.
- Wang, R., Wu, P., Cui, Y., Fizir, M., Shi, J., & He, H. (2020b). Selective recognition and enrichment of sterigmatocystin in wheat by thermo-responsive imprinted polymer based on magnetic halloysite nanotubes. *Journal of Chromatography A*, 460952.
- Wu, A., Zhao, X., Wang, J., Tang, Z., Zhao, T., Niu, L., Yu, W., Yang, C., Fang, M., Lv, H., & Liu, S. (2021). Application of solid-phase extraction based on magnetic nanoparticle adsorbents for the analysis of selected persistent organic pollutants in environmental water: a review of recent advances. *Critical Reviews in Environmental Science and Technology*, 51(1), 44–112.
- Xia, S., Song, Z., Jeyakumar, P., Shaheen, S. M., Rinklebe, J., Ok, Y. S., Bolan, N., & Wang, H. (2019). A critical review on bioremediation technologies for Cr (VI)-contaminated soils and wastewater. *Critical Reviews in Environmental Science and Technology*, 49(12), 1027–1078.
- Xie, Y., Qian, D., Wu, D., & Ma, X. (2011). Magnetic halloysite nanotubes/iron oxide composites for the adsorption of dyes. *Chemical Engineering Journal*, 168(2), 959–963.
- Yamina, A. M., Fizir, M., Itatahine, A., He, H., & Dramou, P. (2018). Preparation of multifunctional PEG-graft-halloysite nanotubes for controlled drug release, tumor cell targeting, and bio-imaging. *Colloids and Surfaces b: Biointerfaces*, 170, 322–329.
- Yang, S., Zong, P., Hu, J., Sheng, G., Wang, Q., & Wang, X. (2013a). Fabrication of β-cyclodextrin conjugated magnetic HNT/iron oxide composite for high-efficient decontamination of U (VI). *Chemical Engineering Journal*, 214, 376–385.

- Yang, W., Jiao, F., Zhou, L., Chen, X., & Jiang, X. (2013b). Molecularly imprinted polymers coated on multi-walled carbon nanotubes through a simple indirect method for the determination of 2, 4-dichlorophenoxyacetic acid in environmental water. *Applied Surface Science*, *284*, 692–699.
- Yendluri, R., Lvov, Y., de Villiers, M. M., Vinokurov, V., Naumenko, E., Tarasova, E., & Fakhruddin, R. (2017). Paclitaxel Encapsulated in Halloysite Clay Nanotubes for Intestinal and Intracellular Delivery. *Journal of Pharmaceutical Science*, *106*(10), 3131–3139. <https://doi.org/10.1016/j.xphs.2017.05.034>
- Yu, L., Wang, H., Zhang, Y., Zhang, B., & Liu, J. (2016). Recent advances in halloysite nanotube derived composites for water treatment. *Environmental Science-Nano*, *3*(1), 28–44. <https://doi.org/10.1039/c5en00149h>
- Yu, M., Wang, L., Hu, L., Li, Y., Luo, D., & Mei, S. (2019). Recent applications of magnetic composites as extraction adsorbents for determination of environmental pollutants. *TrAC Trends in Analytical Chemistry*, *119*, 115611.
- Zain, M. E. (2011). Impact of mycotoxins on humans and animals. *Journal of Saudi Chemical Society*, *15*(2), 129–144.
- Zango, Z. U., Sambudi, N. S., Jumbri, K., Ramli, A., Abu Bakar, N. H. H., Saad, B., Rozaini, M. N. H., Isiyaka, H. A., Osman, A. M., & Suliman, A. (2020). An Overview and Evaluation of Highly Porous Adsorbent Materials for Polycyclic Aromatic Hydrocarbons and Phenols Removal from Wastewater. *Water*, *12*(10), 2921.
- Zare Pirhaji, J., Moeinpour, F., Mirhoseini Dehabadi, A., & Yasini Ardakani, S. A. (2020a). Experimental study and modelling of effective parameters on removal of Cd (II) from water by halloysite/graphene quantum dots magnetic nanocomposite as an adsorbent using response surface methodology. *Applied Organometallic Chemistry*, *34*(7), e5640.
- Zare Pirhaji, J., Moeinpour, F., Mirhoseini Dehabadi, A., & Yasini Ardakani, S. A. (2020b). Synthesis and characterization of halloysite/graphene quantum dots magnetic nanocomposite as a new adsorbent for Pb (II) removal from water. *Journal of Molecular Liquids*, *300*, 112345.
- Zeng, X., Sun, Z., Wang, H., Wang, Q., & Yang, Y. (2016). Supramolecular gel composites reinforced by using halloysite nanotubes loading with in-situ formed Fe<sub>3</sub>O<sub>4</sub> nanoparticles and used for dye adsorption. *Composites Science and Technology*, *122*, 149–154.
- Zhang, A.-B., Liu, S.-T., Yan, K.-K., Ye, Y., & Chen, X.-G. (2014). Facile preparation of MnFe<sub>2</sub>O<sub>4</sub>/halloysite nanotubular encapsulates with enhanced magnetic and electromagnetic performances. *RSC Advances*, *4*(26), 13565–13568.
- Zhang, H., Lai, H., Wu, X., Li, G., & Hu, Y. (2020). CoFe<sub>2</sub>O<sub>4</sub>@HNTs/AuNPs substrate for rapid magnetic solid-phase extraction and efficient SERS detection of complex samples all-in-one. *Analytical Chemistry*, *92*(6), 4607–4613.
- Zhang, R., Zhu, X., Liu, Y., Cai, Y., Han, Q., Zhang, T., & Li, Y. (2019). The Application of Halloysite Nanotubes/Fe<sub>3</sub>O<sub>4</sub> Composites Nanoparticles in Polyvinylidene Fluoride Membranes for Dye Solution Removal. *Journal of Inorganic and Organometallic Polymers and Materials*, *29*(5), 1625–1636.
- Zhang, Y., Tang, A., Yang, H., & Ouyang, J. (2016). Applications and interfaces of halloysite nanocomposites. *Applied Clay Science*, *119*, 8–17. <https://doi.org/10.1016/j.clay.2015.06.034>
- Zheng, P., Du, Y., & Ma, X. (2015). Selective fabrication of iron oxide particles in halloysite lumen. *Materials Chemistry and Physics*, *151*, 14–17.
- Zhitkovich, A. (2011). Chromium in drinking water: Sources, metabolism, and cancer risks. *Chemical Research in Toxicology*, *24*(10), 1617–1629.
- Zhong, S., Zhou, C., Zhang, X., Zhou, H., Li, H., Zhu, X., & Wang, Y. (2014). A novel molecularly imprinted material based on magnetic halloysite nanotubes for rapid enrichment of 2,4-dichlorophenoxyacetic acid in water. *Journal of Hazardous Materials*, *276*, 58–65. <https://doi.org/10.1016/j.jhazmat.2014.05.013>
- Zhou, T., Jia, L., Luo, Y.-F., Xu, J., Chen, R.-H., Ge, Z.-J., Ma, T. L., Chen, H., & Zhu, T. F. (2016). Multifunctional nanocomposite based on halloysite nanotubes for efficient luminescent bioimaging and magnetic resonance imaging. *International Journal of Nanomedicine*, *11*, 4765.
- Zhou, Y., Lu, J., Zhou, Y., & Liu, Y. (2019). Recent advances for dyes removal using novel adsorbents: A review. *Environmental Pollution*, *252*, 352–365.
- Zhu, J., Wei, S., Chen, M., Gu, H., Rapole, S. B., Pallavkar, S., Ho, T. C., Hopper, J., & Guo, Z. (2013). Magnetic nanocomposites for environmental remediation. *Advanced Powder Technology*, *24*(2), 459–467.
- Zhu, K., Duan, Y., Wang, F., Gao, P., Jia, H., Ma, C., & Wang, C. (2017). Silane-modified halloysite/Fe<sub>3</sub>O<sub>4</sub> nanocomposites: Simultaneous removal of Cr (VI) and Sb (V) and positive effects of Cr (VI) on Sb (V) adsorption. *Chemical Engineering Journal*, *311*, 236–246.
- Zhu, X., Li, H., Zhou, H., & Zhong, S. (2015). Fabrication and evaluation of protein imprinted polymer based on magnetic halloysite nanotubes. *RSC Advances*, *5*(81), 66147–66154. <https://doi.org/10.1039/c5ra09740a>
- Zhu, X., Fan, X., Wang, Y., Zhai, Q., Hu, M., Li, S., & Jiang, Y. (2020). Amino modified magnetic halloysite nanotube supporting chloroperoxidase immobilization: enhanced stability, reusability, and efficient degradation of pesticide residue in wastewater. *Bioprocess and Biosystems Engineering*, 1–11.
- Zhu, X., Fan, X., Wang, Y., Zhai, Q., Hu, M., Li, S., & Jiang, Y. (2021). Amino modified magnetic halloysite nanotube supporting chloroperoxidase immobilization: Enhanced stability, reusability, and efficient degradation of pesticide residue in wastewater. *Bioprocess and Biosystems Engineering*, *44*(3), 483–493.

Springer Nature or its licensor (e.g. a society or other partner) holds exclusive rights to this article under a publishing agreement with the author(s) or other rightsholder(s); author self-archiving of the accepted manuscript version of this article is solely governed by the terms of such publishing agreement and applicable law.